JOURNAL OF GEOPHYSICAL RESEARCH, VOL. 108, NO. E12, 8076, doi:10.1029/2002JE002026, 2003

Exploring Gusev Crater with Spirit: Review of science objectives and testable hypotheses

Nathalie A. Cabrol,[1] Edmond A. Grin,[1] Michael H. Carr,[2] Brad Sutter,[1] Jeffrey M. Moore,[1] Jack D. Farmer,[3] Ronald Greeley,[3] Ruslan O. Kuzmin,[4] David J. DesMarais,[1] Marc G. Kramer,[1] Horton Newsom,[5] Charles Barber,[5] Ivan Thorsos,[5] Kenneth L. Tanaka,[6] Nadine G. Barlow,[7] David A. Fike,[8] Mary L. Urquhart,[9] Brian Grigsby,[10] Frederick D. Grant,[11,12] and Olivier de Goursac[13]

Received 5 December 2002; revised 28 August 2003; accepted 3 September 2003; published 30 December 2003.

[1] Gusev Crater was selected as the landing site for the Mars Exploration Rover (MER) Spirit mission. Located at the outlet of Ma'adim Vallis and 250 km south of the volcano Apollinaris Patera, Gusev is an outstanding site to achieve the goals of the MER mission. The crater could have collected sediments from a variety of sources during its 3.9 Ga history, including fluvial, lacustrine, volcanic, glacial, impact, regional and local aeolian, and global air falls. It is a unique site to investigate the past history of water on Mars, climate and geological changes, and the potential habitability of the planet, which are central science objectives of the MER mission. Because of its complex history and potential diversity, Gusev will allow the testing of a large spectrum of hypotheses with the complete suite of MER instruments. Evidence consistent with long-lived lake episodes exist in the landing ellipse area. They might offer a unique opportunity to study, for the first time, Martian aqueous sediments and minerals formed in situ in their geological context. We review the geological history and diversity of the landing site, the science hypotheses that can be tested during the MER mission, and the relevance of Gusev to the MER mission objectives and payload. *INDEX TERMS:* 6225 Planetology: Solar System Objects: Mars; 5470 Planetology: Solid Surface Planets: Surface materials and properties; *KEYWORDS:* Gusev, lake, Apollinaris Patera, Spirit rover

Citation: Cabrol, N. A., et al., Exploring Gusev Crater with Spirit: Review of science objectives and testable hypotheses, *J. Geophys. Res.*, *108*(E12), 8076, doi:10.1029/2002JE002026, 2003.

1. Introduction

[2] The MER landing sites have been selected in order to maximize the mission science return within the constraints of the Mars Exploration Project (MEP), which include engineering constraints, schedule and payloads (Mars Exploration Program, MER PIP, August 2001) [*Golombek et al.*, 2001]. The goal for each rover mission is to determine the aqueous, climatic, and geologic history of a site on Mars where conditions may have been favorable for the preservation of evidence containing possible prebiotic or biotic processes. While encompassing a wide range of possible settings that include former fluvial, lacustrine and/or hydrothermal environments, clear evidence for surface processes involving ancient water was the main scientific criteria used in the identification and selection of the two final landing sites. Out of 185 candidates, Gusev crater and Meridiani Planum (a.k.a. the Hematite) were finally selected as the landing sites for, respectively, the Spirit and Opportunity rovers after two years of down selection. At Gusev the evidence for past water action is morphological with the large Ma'adim Vallis entering the crater basin, whereas at Meridiani Planum, the presence of the mineral hematite is consistent with the existence of an ancient aqueous environment. This paper focuses on Gusev crater.

[3] Gusev Crater is a 150 km diameter impact basin that collected flows from the 900 km long Ma'adim Vallis, as well as depositional inputs from Apollinaris Patera, an ancient volcano located 250 km to the North. The unique geological setting of Gusev Crater makes it an outstanding

[1]NASA Ames Research Center, Moffett Field, California, USA.
[2]U.S. Geological Survey, Menlo Park, California, USA.
[3]Department of Geological Sciences, Arizona State University, Tempe, Arizona, USA.
[4]Vernadsky Institute, Russian Academy of Sciences, Moscow, Russia.
[5]Institute of Meteoritics and Department of Earth and Planetary Sciences, University of New Mexico, Albuquerque, New Mexico, USA.
[6]Department of Physics and Astronomy, Northern Arizona University, Flagstaff, Arizona, USA.
[7]U.S. Geological Survey, Flagstaff, Arizona, USA.
[8]Department of Earth, Atmospheric, and Planetary Sciences, Massachussetts Institute of Technology, Cambridge, Massachusetts, USA.
[9]Department of Science and Mathematics Education, University of Texas at Dallas, Richardson, Texas, USA.
[10]Schreder Planetarium, Redding, California, USA.
[11]Department of Geology, University of Mississippi, Jackson, Mississippi, USA.
[12]Now at Department of Geological Sciences, Arizona State University, Tempe, Arizona, USA.
[13]Mars Society en France, Suresnes, France.

0148-0227/03/2002JE002026

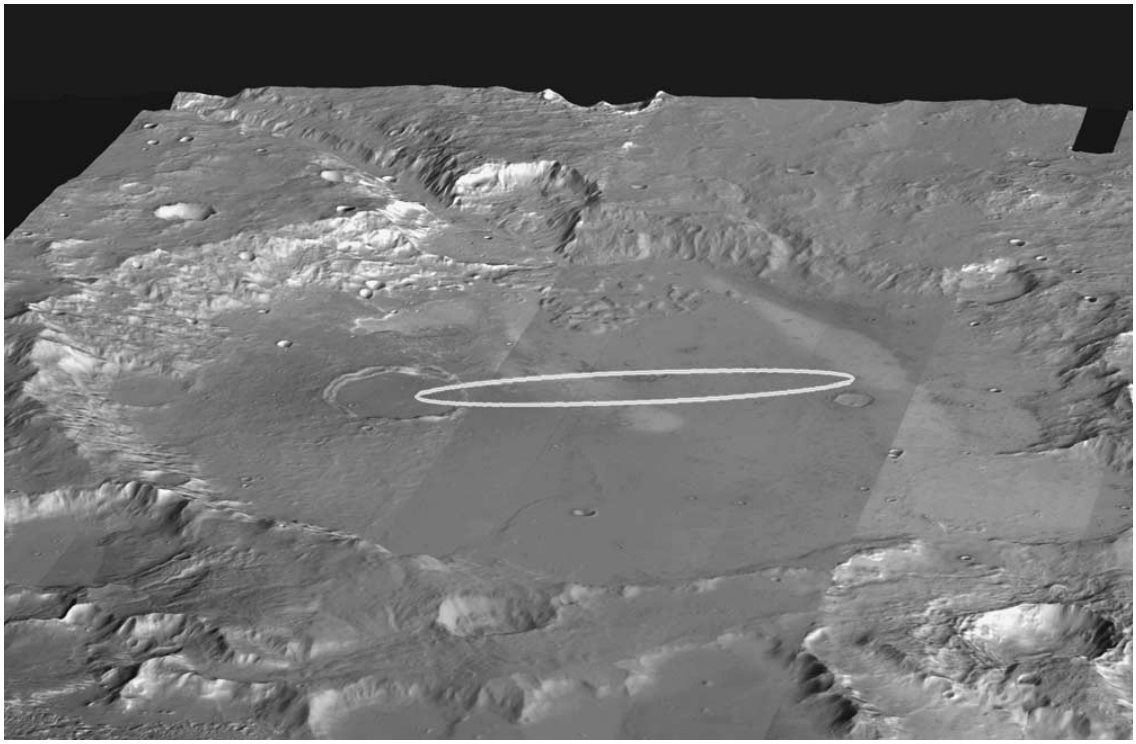

Figure 1. Map of Gusev and the MER A landing ellipse with part of MOC narrow-angle high-resolution image coverage. The central region of the ellipse has the greatest probability of landing. The central region is located at the lowest part of Gusev and shows numerous layered deposits of various albedo, potential rover access to outcrop, and varied landforms. The ellipse is at the distal end of the Ma'adim Vallis deltaic region. By comparison with terrestrial lake bed analogs, this region is a favorable location for the preservation of fossil records.

candidate site for addressing the overarching MEP goal to "follow the water" (E. Weiler, NASA, 2003). In this paper we also show that Gusev Crater is an excellent site for addressing the key science objectives of the MER mission. Since Viking, Gusev Crater has been hypothesized to have been a locus for prolonged fluvial and lacustrine activity [*Cabrol and Grin*, 1995; *Cabrol et al.*, 1998a, 1998b; *Grin and Cabrol*, 1997]. These earlier hypotheses have been strengthened by new data returned from Mars Global Surveyor (MGS) and Mars Odyssey (MO). Moreover, the prolonged (~3.9 Ga) depositional history of Gusev Crater provides access to a potentially wide diversity of depositional processes and products, including (a) fluvial and/or glacial deposits derived from a wide variety of parent rock units exposed in the watershed of Ma'adim Vallis, a catchment area of several million square kilometers [*Irwin et al.*, 2002]; (b) volcanic materials (e.g., air fall tuffs, pyroclasts) originating from Apollinaris Patera; (c) globally derived atmospheric dust deposits; (d) coarser-grained wind-deposited material derived from local and regional sources [*McCauley*, 1973]; (e) ejecta deposits from regional impacts, and (f) aqueous sediments deposited by streams or lakes. The diversity of geologic processes that appear to have affected Gusev Crater over its long history and potentially extensive depositional record, suggests an unprecedented opportunity to learn about the history of water, climate and potential habitability of Mars [*Farmer*, 1995]. The varied interpretations that have been offered by previous workers to explain the features and geologic history of Gusev Crater define a set of multiple working hypotheses that are amenable to testing using the rover payload.

[4] The following sections review (a) the science questions that have been raised by previous works to explain Gusev's geologic history; (b) the hypotheses developed after the Viking missions; (c) how these hypotheses have fared with the arrival of the data from recent missions; (d) what new hypotheses are suggested by observations and results from MGS and MO; and (e) how to test these hypotheses with the MER payload and within the range of a rover mission traverse.

2. Geological Context

[5] The study of geological units in the watershed region of Ma'adim provides critical information for understanding the nature of the parent rocks which provided sediments to the floor of Gusev Crater and which will be accessible within the MER landing site area (Figure 1). Regional investigations were carried out by *Tanaka* [1986] *Greeley and Guest* [1987], *Kuzmin et al.* [2000] and *Hartmann and*

Neukum [2001] using Viking data and Mars Orbiter Camera (MOC) images. More recently, *Irwin et al.* [2002] and M. Kramer et al. (manuscript in preparation, 2003) have revisited earlier interpretations using MOC, Mars Orbiter Altimeter (MOLA) and Mars Orbiter (MO) data. This previous work, which is reviewed in the following sections, provides a context for understanding the geologic history of the Gusev Crater and surrounding terrain.

2.1. Noachian Stratigraphy

[6] The Ma'adim Vallis/Gusev crater system dissects cratered highland rocks of Middle Noachian age [*Greeley and Guest*, 1987] thought to be about 3.9 Ga old [*Tanaka*, 1986; *Hartmann and Neukum*, 2001]. This age is based on the density of craters larger than 16 km in diameter apparent in Viking images [*Tanaka*, 1986; *Hartmann and Neukum*, 2001]. Using MOLA topographic data, *Frey et al.* [2002] have recorded a population of large ''quasi-circular depressions'' (QCD's) thought to be the expression of buried impact basins. The QCD's summed with the surface population correspond to an age of Early Noachian that likely represents materials dating back to solidification of the crust and heavy bombardment, ~4–4.6 billion years ago.

[7] Noachian rocks and surfaces have been modified by complex active processes at various degrees until recent times [*Tanaka et al.*, 1988]. Because of the antiquity of exposure of the surface, impact gardening has churned up the upper several hundred meters to a couple kilometers of this material, with more intense grinding and thus finer material near the surface to form a megaregolith, similar to that found on the Moon [*Hartmann et al.*, 2001]. Impacts, magmatism, tectonism, metamorphism (including hydrothermal alteration), erosion, weathering, and sedimentation following crustal solidification have likely served to greatly complicate the detailed lithologic makeup of the Noachian crust. Local layering and light-colored rocks exposed in ancient highland scarps may be indicative of sedimentary deposits collected within crater floors and intermontane basins [*Malin and Edgett*, 2000b]. In the walls of Valles Marineris, layers tens of meters thick [*Malin and Edgett*, 2000a] forming sequences of up to several kilometers may be stacks of mechanically weathered basalt flows [*McEwen et al.*, 1999] that lie below exposures of Noachian rocks exposed on the adjacent plateaus [*Witbeck et al.*, 1991]. Other Noachian layered materials may include volcanic ash deposits [*Tanaka*, 2000]. Igneous intrusions in the form of dikes and stocks likely formed locally and may have driven hydrothermal circulation.

[8] The occurrence of valley networks across Mars during the Late Noachian (~3.7–3.8 Ga) indicates that atmospheric precipitation and/or near-surface groundwater discharge reworked the Noachian surface at that time [e.g., *Carr and Malin*, 2000], and fluids may have circulated extensively through more permeable parts of the crust. As heat flow and impact bombardment declined and the upper crust generally remained at subfreezing temperatures, a deepening cryosphere developed, eventually reaching a few kilometers in depth [*Clifford*, 1993; *Clifford and Parker*, 2001]. This cryosphere likely developed after all or the majority of Ma'adim Vallis dissection. However, recent gully formation in middle and high-latitude areas on Mars [*Malin and Edgett*, 2000a] indicates that near-surface water in the crust may have occurred at least episodically through geologic time [*Mangold et al.*, 2002; *Hartmann et al.*, 2002]. Alternatively, the gullies may represent erosion produced by CO_2 discharge [*Musselwhite et al.*, 2001], although *Stewart and Nimmo* [2001] argue that CO_2 is too unstable to produce the gullies. Other hypotheses to explain the formation of the gullies have been presented. They include: avalanches of rocks and debris or dust [*Bulmer et al.*, 2002], and the melting of ice and snowpacks [*Lee et al.*, 2002; *Christensen*, 2003].

[9] The processes operative during the Noachian could have produced a myriad of primary lithologies, weathering products, secondary mineralization, structures, and textures. The exposed Noachian geology in the Ma'adim/Gusev region provides clues to some of these processes (see next sections), but much of the Noachian geologic record remains obscure.

[10] The oldest terrain associated with the Noachian in the Ma'adim region corresponds to mountainous material and could consist of impact breccias and ancient volcanic massifs dating back from to the period of late heavy bombardment. As they are bounded by cliffs and faults, it has been proposed by *Scott and Tanaka* [1986] that these units were subsequently uplifted by faulting. Early Noachian units include curvilinear ridges with sharp ridges and grooves representing degraded impact crater rim material or possibly ancient volcanic constructs. They are embayed by younger channels and basin floor materials. The Middle Noachian degraded rims are buried under these younger materials and visible only on local exposures due to exhumation processes. The Late Noachian sees the first record of sedimentation associated with flooding from the precursor to Ma'adim Vallis. During this period, water derived from small valley networks on the eastern and southern portion of Gusev's rims may have ponded in Gusev [*Kuzmin et al.*, 2000], see Figure 2.

2.2. Hesperian Stratigraphy

[11] The Hesperian system in the Ma'adim Vallis/Gusev region is the richest in terms of the record of units and associated processes. Eruptions of Apollinaris Patera can be traced back to the early part of the Hesperian with pyroclasts and lava flows deposited north and northwest of Gusev. This is also when Ma'adim Vallis is carved and provides sediments to Gusev [*Kuzmin et al.*, 2000]. This activity continues throughout the Late Hesperian with potential intravalley lake occurrences in the downstream region of Ma'adim Vallis [*Cabrol et al.*, 1996].

2.3. Amazonian Stratigraphy

[12] Activity in the Ma'adim Vallis/Gusev crater system extends to the Early Amazonian where the possible record of late fluvio-lacustrine episodes are still observed but are reaching their final stage. The most recent flow deposits are clearly produced by Ma'adim Vallis. Tongue-like lobe morphologies with sinuous margins suggest that glaciation processes occurred at this time in the region. By Middle to Late Amazonian the fluvial and lacustrine activity seem to have ceased completely. Glacial to subglacial conditions were suggested by *Grin and Cabrol* [1997] from deltaic morphologies in Gusev that resemble Antarctic subglacial deltas and an esker-like formation in the upstream section of Ma'adim [*Carr*, 1996]. After the Middle Amazonian,

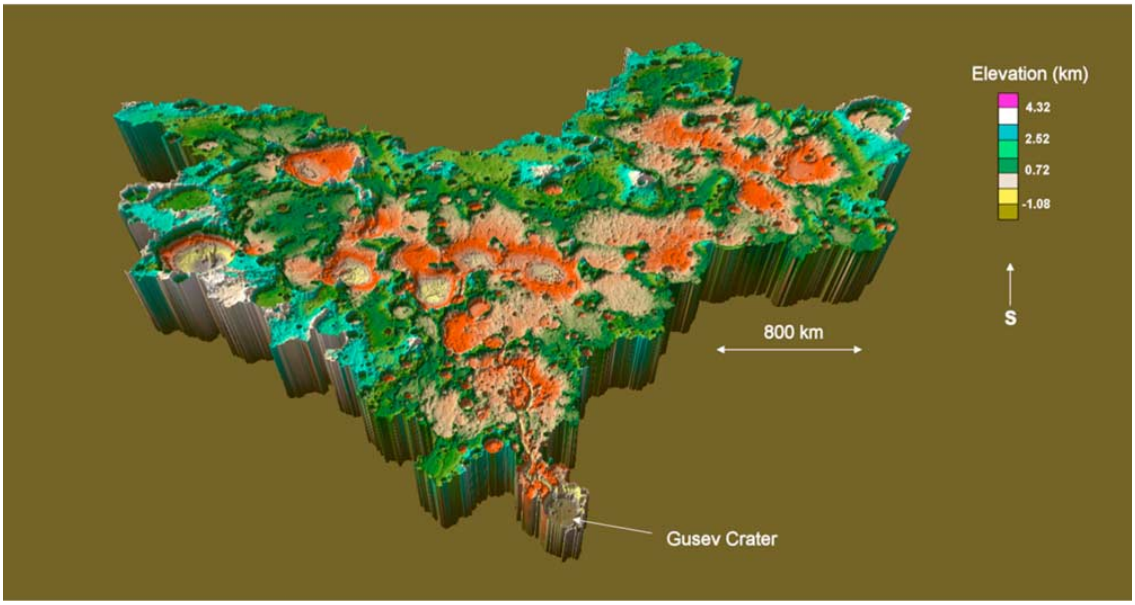

Figure 2. Ma'adim Vallis watershed as reconstructed using the MOLA data. Its size is comparable to the largest terrestrial watersheds (e.g., Amazon basin). A series of basins connect to the main hydrographic system, which empties in Gusev. The topography and morphology seem to indicate that they were a series of closed basins rather than a giant one and that ice/snow played a substantial role in their activation.

aeolian processes become dominant in shaping the landscape.

3. New Data and Observations

[13] MGS and MO have returned high-resolution data which have led to several new hypotheses for both Gusev and Ma'adim. They are reviewed below with the exception of the THEMIS results for Gusev which are discussed by *Milam et al.* [2003].

3.1. Fluvial-Lacustrine Context of Gusev

[14] Gusev Crater was selected because of evidence that water once ponded within the crater and partly filled the crater with sediments. Over thirty years ago, it was recognized that the heavily cratered highlands of Mars are dissected by branching valley networks, probably as a result of slow erosion by running water [*Masursky*, 1973]. Other much larger channels were attributed to large floods [*Baker and Milton*, 1974] and termed outflow channels [*Sharp and Malin*, 1975]. Subsequent detailed mapping showed that while almost all regions of the cratered highlands are dissected by valley networks, large integrated drainage systems are rare. Most of the drainage is into local lows so that for over ninety percent of the networks the longest path through the system is under 200 km [*Carr and Clow*, 1981; *Carr*, 1995]. Commonly, these networks are separated by areas where no dissection can be discerned. This appears to be an intrinsic property of the drainage system although in some places the absence of obvious dissection may result in part from resolution, as suggested by early results from THEMIS (P. R. Christensen, personal communication, 2002), or from degradation as a consequence of the networks' old age. Major exceptions to this local pattern of dissection are the Loire-Parana system in Margaritifer Terra, Reull Vallis that drains into Hellas and Ma'adim Vallis that feeds into Gusev crater.

[15] The disjointed drainage system is in part a reflection of the surface topography. Most regional slopes in the cratered highlands are down toward the northern plains, or into Argyre and Hellas [*Carr*, 1995; *DeHon*, 2001] and the regional drainage pattern is consistent with these slopes. However, superimposed on these gentle regional slopes are numerous closed basins so that through-going valleys that extend large distances down the regional slopes are rare. The superimposed closed basins occur on all scales from the 2000 km diameter impact basin Hellas down to small impact crater. In addition to the obvious impact craters, there are quasi-circular depressions that appear to be ancient degraded impact basins [*Frey and Schultz*, 1988] and degraded-shaped depressions that result from volcanic and tectonic activity.

[16] The cratered uplands to the south of Ma'adim Vallis have many of the attributes just described. Figure 3 outlines several geomorphic elements of the terrain to the south of Ma'adim Vallis that might have affected the origin and evolution of the valley and hence the crater Gusev. *Irwin et al.* [2002], using MOLA data, outlined a possible drainage basin that drains through Ma'adim. Precipitation falling anywhere within this basin would drain through Ma'adim Vallis into Gusev Crater, provided that all closed basins along the drainage pathways are filled (i.e., lakes were

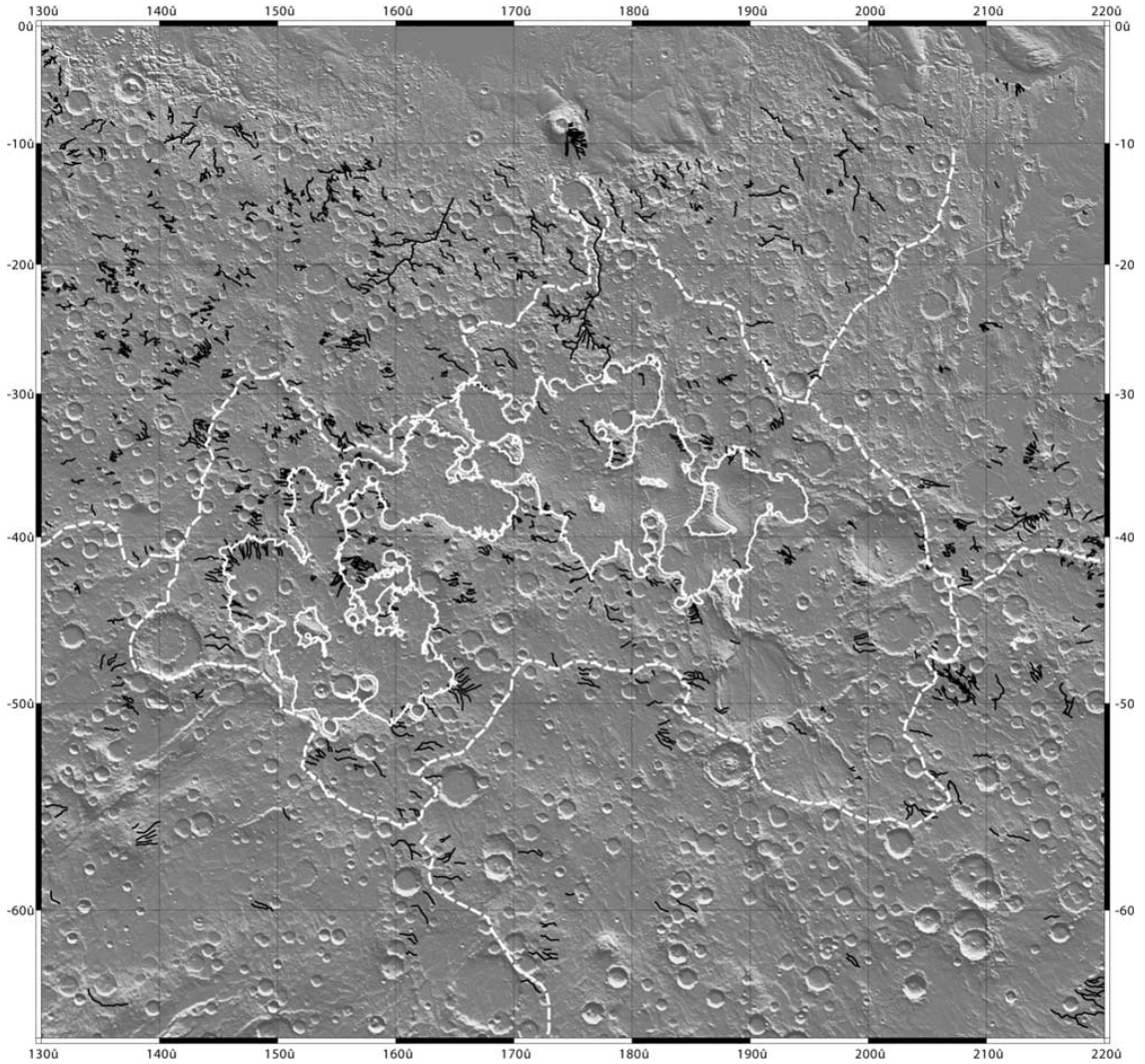

Figure 3. Drainage features in the cratered uplands south of the Gusev crater. The dashed white lines are major drainage divides. Solid white lines outline closed basins. The black lines are the valley networks.

present within the inner basins). Southwest of the Ma'adim drainage basin, flow is northwest into the Hellas basin, and northeast flow is into the northern plains most through small valleys such as Al Qahira. To the east, flow is through Mangala Valles. The distribution and/or occurrence of precipitation at the time of the formation of Ma'adim Vallis are both unknown, the implication of a surface drainage divides for groundwater flow is uncertain. (For example, if the source of groundwater is from basal melting of the polar caps, as suggested by *Clifford* [1987], then the local topography would have exercised little control over the directions of groundwater flow.)

[17] A crucial issue with respect to the origin of Ma'adim is whether the local basins within the larger Ma'adim drainage basin did in fact contain lakes so that Ma'adim was fed by a significant fraction of the outlined basin. *Irwin et al.* [2002] present evidence that a large paleolake was present upstream at the time of or just prior to the formation of Ma'adim Vallis. The lake was dammed behind a 1100 m high ridge that is part of the rim of a large, degraded impact crater (Figure 4). They suggest that the lake spilled over the ridge at 38°S/177°E, rapidly lowering the lake level from 1100 to 950 m, the elevation of the present outlet. This release over 100,000 km^3 of water which cut Ma'adim Vallis and deposited part of the resulting erosional debris in Gusev Crater. As the lake level lowered, the smaller subsidiary basin shown in Figure 3 would have become isolated, and in the final stages of outflow only the 950 m basin would have drained through the gap at 38°S/177°E into Ma'adim Vallis. As supporting evidence for the former presence of the lake, *Irwin et al.* [2002] list (1) breaks in slope at the 1100 m level, (2) widening of the valley that drains into the depression at

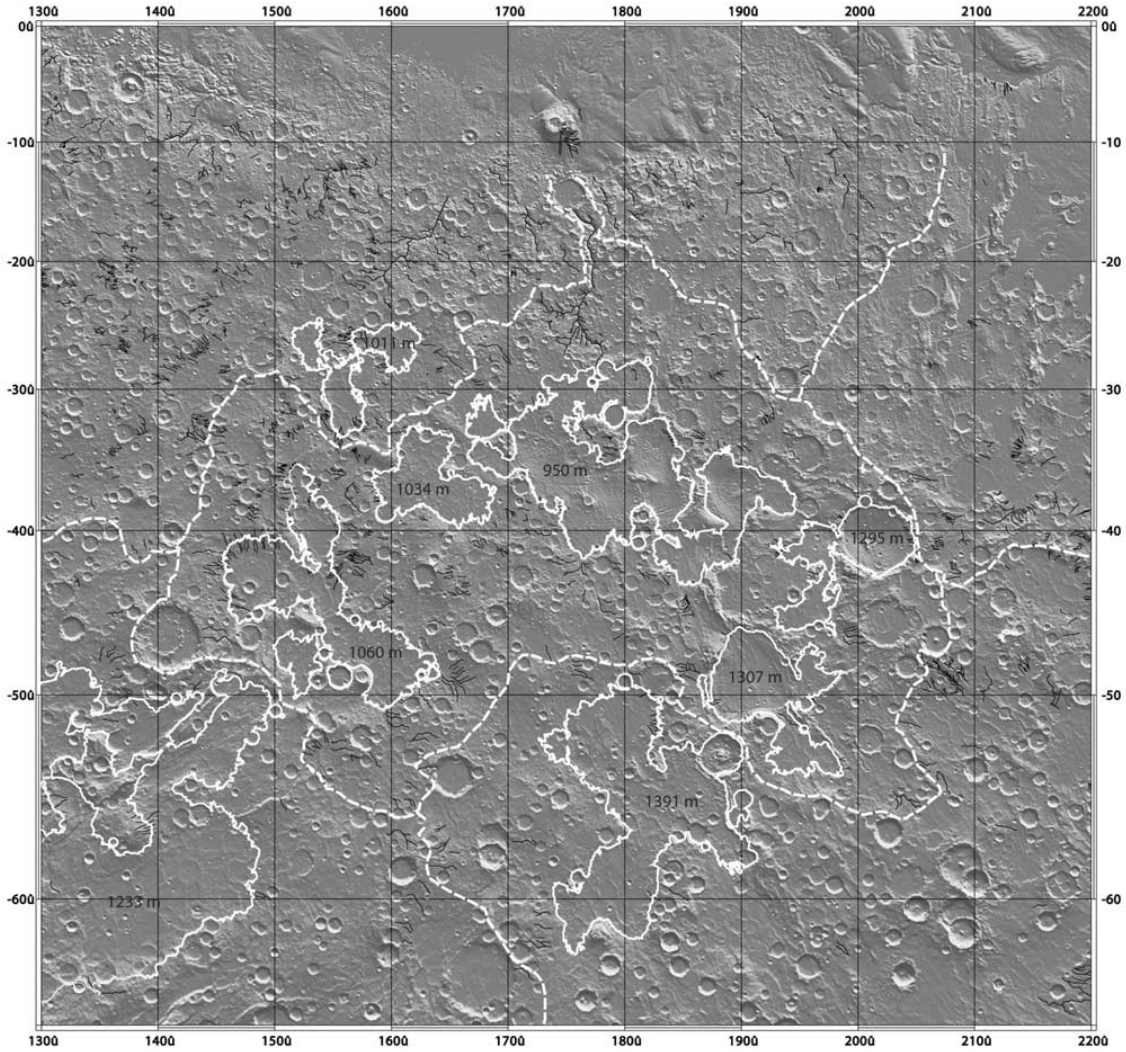

Figure 4. Same as in Figure 3, except that the dashed white line outlines the 1100 m shoreline of the lake hypothesized by *Irwin et al.* [2002]. Solid white lines outline closed basins, each with an outlet elevation, as indicated.

the 1100 m level, (3) absence of valleys below the 950 m level, (4) terraces within some basins, as at 38S/185E, (5) clusters of low hills, such as the Gorgonum and Atlantis Chaos in the deepest parts of some basins, and (6) the bowl-shaped nature of the subsidiary basins, in contrast to the normally flat floors of most highlands craters, (an attribute that they suggest results from lacustrine rather than fluvial sedimentation). The floor of the proposed lake and the floors of Gusev Crater and Ma'adim Vallis all appear to be of similar age (Late Noachian), consistent with a common origin. The general scarcity of valleys within the area of the proposed lake is evident from Figure 3. The only place where there are a significant number of valleys within the lake area is around 42°S/146°E and these terminate at the 950 m level.

[18] While there is good evidence in support of the former lake and its drainage through Ma'adim, many issues remain uncertain. These include: was the draining of the lake to the 950 m level gradual or catastrophic? How long the lake was in existence and what climatic conditions prevailed after the level fell to the present outlet level? Where the water came from? The absence of bed forms on the floor of Ma'adim and Gusev (longitudinal scour, cataracts, streamlined islands, etc.) suggests that Ma'adim was not cut catastrophically by a stream with dimensions comparable to the present valley bed-like a typical outflow channel but was instead cut slowly by a stream with dimensions much smaller than the present channel. This is consistent with the lake hypothesis in that the outlet to the lake at 38°S/177°E has a much smaller cross section than the lower reaches of Ma'adim. *Cabrol et al.* [1998b]. The outlet itself is unlikely to have ever been filled with water since the water level would have dropped as the outlet was eroded

deeper. Slow erosion of Ma'adim is also consistent with the presence of numerous tributaries that were not supplied by the postulated lake. *Cabrol et al.* [1998b] and *Kuzmin et al.* [2000], on the basis of terraces at different levels on the walls of Ma'adim and their dissection by tributaries, argued for an episodic formation of Ma'adim, with episodes of slow erosion being spread over an extended period of time (from late Noachian to early Amazonian).

[19] The lake hypothesis provides little insight into the prevailing climatic conditions or the source of the water. *McKay et al.* [1985] have shown that, even under present climatic conditions, ice covered lakes could survive on Mars for extended periods of time provided that losses by sublimation from the ice surface are replaced. In the absence of precipitation, sublimation losses could be replaced by groundwater seepage, thereby maintaining a lake level consistent with the surrounding groundwater table. Even if tributary bed forms below the range of the typical resolutions of 1.5–12 m/pixel could not be seen, the scarcity of valleys, at the resolution of MOC, MGS and/or MO data sets, feeding into the lakes (Figures 3 and 4) supports the supposition that the lakes were fed mainly by groundwater. Groundwater seepage cannot, however explain all the features of the Ma'adim drainage basin. Many of the valley networks portrayed in Figure 3 are at elevations in excess of 2000 m. In the absence of precipitation, the only plausible way to sustain groundwater at high elevation level drainage northward down the regional slope is by introduction of water into the ground by basal melting at the poles [*Clifford*, 1987; *Clifford and Parker*, 2001]. Yet, *Carr* [2002] shows that only a small fraction of the cratered terrain beneath the south polar deposits reaches an elevation of 2000 m. Valley networks at elevations in excess of 2000 m are thus very unlikely to have formed by groundwater seepage. Some form of precipitation was likely involved. If the low drainage density evident from Figure 3 is a primary drainage feature, and not due to obscuration of valleys by later burial and erosion, then it is unlikely that the area experienced precipitation over extended periods of time. Given that precipitation was needed to cut at least the valleys over 2000 m in elevation, the precipitation may have resulted from rare episodes, as at high obliquities [*Jakosky and Carr*, 1985] or following formation of large outflow channels [*Baker*, 2001]. The lower elevation valleys and the postulated lakes all could have been fed largely by groundwater, as a consequence of polar basal melting.

[20] There are, however, several observations showing that the hypothesis of one giant paleolake is only one among several possible scenarios that could explain the configuration of the upstream region. The first observation comes from the ages that are provided by *Irwin et al.* [2002] for the floor of Gusev, Ma'adim, and the basin in the Ma'adim upstream region. *Cabrol et al.* [1998b] and *Kuzmin et al.* [2000] in two separate studies came to converging ages of Late Hesperian to Early Amazonian for the most recent fluvio-lacustrine deposits in Gusev based on N(2), N(5), and N(16) diameter populations of superimposed impact craters. Those deposits could be divided into three stages ranging in age from Early Hesperian to Early Amazonian. The formation of Gusev Crater itself is Early Noachian as suggested by crater count [*Tanaka*, 1986; *Hartmann and Neukum*, 2001]. The floor of Ma'adim Vallis shows the same crater density values as the most recent fluvio-lacustrine deposits in Gusev (i.e., Late Hesperian to Early Amazonian). The results by *Cabrol et al.* [1998b] and *Kuzmin et al.* [2000] argue against the theory of only one episode of a giant Noachian lake and MOLA is clearly showing that there are basins upstream of Ma'adim as suggested by *Irwin et al.* [2002]. Understanding their extent, origin (e.g., water, ice, or other), physiography (connected versus closed) and their activity through time (one unique episode versus a series of active episodes following cycles) is critical for the formulation of geological hypotheses that can be tested by the MER payload.

[21] The highlands region potentially could have delivered substantial quantities of water/ice and sediments through the upstream paleolake(s).The total size of the highlands area draining into Gusev Crater is 7M Km^2, which is as big as the largest terrestrial drainage basins in the Amazon and Congo Basins. Possible sources of water for surface water/ice flow activity in the highlands include glacial/ice sheet, subsurface aquifers, hydrothermal activity and precipitation. If material was ever delivered into Gusev from the surrounding highlands via surface flow, the duration that these water/ice flows (and associated movement of sediments) were active and surface area over which they occurred remain unclear. M. Kramer et al. (manuscript in preparation, 2003) are evaluating four possible surface water and ice flow scenarios across the highlands region near Gusev. In two of these scenarios, potential water bodies ranging in size from the equivalent of the Mediterranean sea [*Irwin et al.*, 2002] up to 1.5 M Km^2 may be prevalent. In another scenario, 58,000 Km^2 (Great Lakes-sized water bodies, Michigan, USA) closed basins with ice/glacial activity may have persisted. Closed basins in the highlands region may have provided a source of groundwater to the Gusev region. An alternative scenario that ground water/subsurface water dynamics have dominated the history of the highlands is also considered. The presence of periglacial features (polygonal ground, collapse features and possibly pingos) in the deepest portions of several large highlands depressions suggests that ice may be implicated in the history of surface water flows in this region. The many incised stream features draining into these depressions also suggest surface water flow.

3.2. Single-Layered Ejecta and Pedestal Craters

[22] MOC images within Gusev Crater, the landing ellipse, and the Ma'adim Vallis region point toward the possible presence of an exceptionally volatile-rich layer near the surface which may exist to the present time [*Barlow*, 2003]. The landing ellipse within Gusev contains large numbers of small (10s of meters diameter) craters. Most of these craters have been modified by aeolian processes, as indicated by the abundance of sand dunes on the infilled floors. As a result, few of the characteristics of pristine craters can be discerned within the landing ellipse. Spirit may not land within roving distance of a fresh ejecta blanket where it could sample material excavated from depth within the Gusev deposits. However, if such ejecta deposits can be accessed, or if weathered products from older eroded ejecta blankets can be identified within the sampled material, information about the near-surface material (within a few tens to hundreds of meters depth) could be obtained.

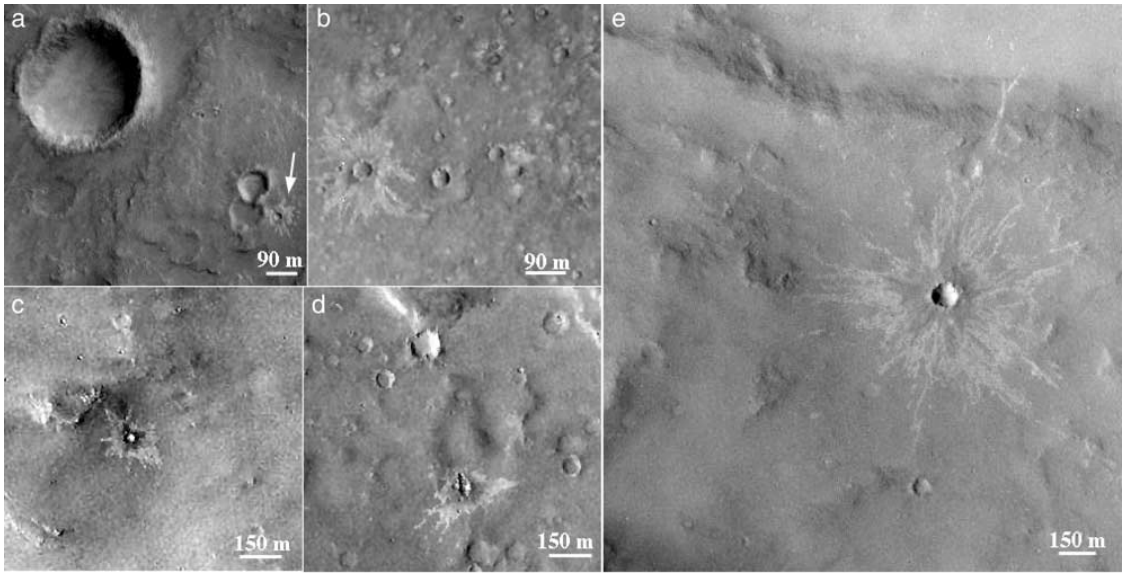

Figure 5. SLE and pedestal craters in Gusev ellipse and Ma'adim. One of the most promising results provided by MGS in the Gusev and Ma'adim region was the discovery of SLE and pedestal craters of small diameter that could indicate the presence of volatile-rich material very close to the surface (<10 m). If this is the case, there could be a unique opportunity in Gusev to study the interaction between near-surface ice and atmosphere as well as the role of ice in the shaping of the landscape (e.g., cryokarst). (a) 50 m diameter pedestal crater in Gusev crater (MOC image E1201240); (b) 80 m diameter SLE crater in Gusev, with large ejecta located 1 km north of central ellipse margin (MOC image E05-03287); (c-e) examples of the numerous pedestal and SLE impact craters in the region of Ma'adim Vallis (MOC images MO8-03444 (Figures 5c and 5e) and M10-02644 (Figure 5d)). This region appears potentially richer in volatile than expected for this latitude. Courtesy of NASA/JPL/Malin Space Science Systems.

[23] The layered (formerly called "fluidized," "lobate," or "rampart" [see *Barlow et al.*, 2000] ejecta morphologies displayed within the landing ellipse are dominated by the single layer ejecta (SLE) morphology, in which one ejecta layer surrounds the crater (Figure 5). Previous studies based on Viking imagery suggested that the smallest craters displaying a SLE morphology in this region were about 4 km in diameter [*Kuzmin et al.*, 1988]. On the basis of analysis of narrow-angle MOC imagery, the smallest craters with an unambiguous SLE morphology within Gusev are about 50 m in diameter. Many studies have argued that the SLE morphology is the result of impact into ice-rich materials [*Mouginis-Mark*, 1979, 1981; *Costard*, 1989; *Barlow and Bradley*, 1990; *Baratoux et al.*, 2002] (S. T. Stewart et al., Impact processing and redistribution of near-surface water on Mars, submitted to *Nature*, 2002, hereinafter referred to as Stewart et al., submitted manuscript, 2002). *Garvin and Frawley* [1998] have determined that the depth (d) of minimally degraded simple craters (<7–8 km diameter) as a function of diameter (D) is given by $d = 0.14D^{0.90}$. Using this relationship, the smallest SLE craters in Gusev excavated to depths of approximately 10 m. This value should be considered an average estimate for the depth of the ice-rich layer creating the SLE morphology. If the craters measured by *Garvin and Frawley* [1998] have been infilled even slightly, the depths will be underestimates of the true excavation depth of the crater, indicating that the ice could lie at greater depths (but no deeper than the current diameter of the crater, which is about 50 m). Alternately, computer simulations by *Baratoux et al.* [2002] and Stewart et al. (submitted manuscript, 2002) suggest that a certain concentration (around 20%) of volatiles is necessary in the soil before the SLE morphology is produced. Therefore ice might exist closer to the surface but the necessary concentrations are not reached until one approaches the 10 m depth. In any case, the small diameters associated with SLE craters suggest that Gusev deposits are ice-rich even close to the surface. If Spirit is able to access fresh ejecta deposits, it could test this hypothesis by searching for evidence of hydrated minerals.

[24] Another indicator that the material within Gusev could be ice-rich comes from the number of pedestal craters found in this region. Pedestal (Pd) craters are craters with ejecta blankets which are perched above the level of the surrounding terrain (Figure 5). *McCauley* [1973] and *Arvidson et al.* [1976] proposed that the pedestal morphology results from the ejecta acting like an armor, preventing the underlying material from being removed during periods of aeolian deflation. The pedestal craters seen within Gusev tend to be distributed within regions where other evidence of wide-scale deflation is seen, such as isolated buttes and the eroded edges of the central deposit. Studies of the latitudinal distribution of Pd craters from Viking imagery suggest that these craters are more common within high-latitude regions which display other indicators of ice-rich deposits [*Costard*, 1989; *Ramstad*, 2001]. *Ramstad* [2001] measured the ejecta

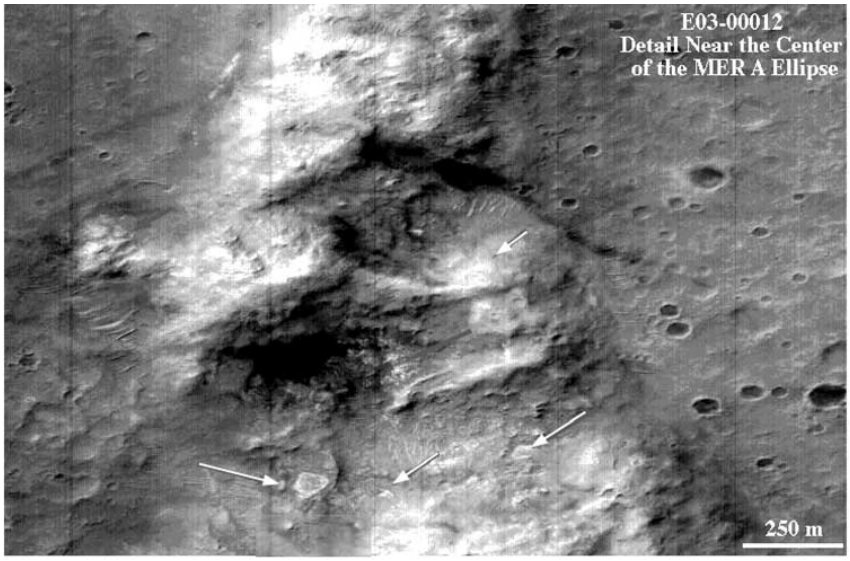

Figure 6. Layers and diversity of material in the central region of the Gusev landing ellipse. The white arrows indicate bright albedo exposures of material that stand out compared to the average local albedo. They are observed in an environment of very thin layering that can be seen in this image. Their contours follow that of the layers in many instances. They could have resulted from depositional processes and indicate materials of different origins and/or various stages of weathering in similar materials. Courtesy of NASA/JPL/Malin Space Science Systems.

mobility ratio (EM = maximum extent of ejecta flow/crater radius) of Pd and SLE craters and found that while Pd craters are typically smaller than SLE craters, they also display greater EM. This is consistent with what we see in Gusev: Pedestal craters typically range from 30 to 50 m in diameter and display EM values between 2.0 and 5.5 while SLE craters are larger than 50 m in diameter and show EM values between 1.0 and 1.7. The ejecta mobility ratio is commonly cited as evidence for incorporation of volatile-rich material within the ejecta and thus suggests that higher EM values are the result of higher concentrations of volatiles in the target material [*Mouginis-Mark*, 1979; *Costard*, 1989; *Barlow and Pollak*, 2002]. On the basis of the distribution and physical characteristics of Pd craters, this morphology is likely produced by crater formation in a fine-grained, ice-rich deposit which is subsequently deflated from the surrounding terrain. This model could explain the observation by *Garvin et al.* [2000] that the volume of material in the pedestal ejecta blanket is greater than the volume of the crater itself; the current ''ejecta blanket'' would contain not only the actual ejecta but also material from the original deposit which was armored against the effects of aeolian deflation by the emplacement of the ejecta blanket.

3.3. Diversity of Deposited and Eroded Layered Materials in the Landing Ellipse

[25] MOC coverage of Gusev as part of the landing site selection effort has provided new observations that broaden the spectrum of hypotheses that could be tested in situ. At high resolution, the floor of Gusev appears to be intensely layered (Figures 6 and 7) over a significant portion of the landing ellipse, especially in the central region where the rover has the greatest probability of landing. The layers in Gusev are much thinner than those described by *Malin and Edgett* [2000b]. The layering occurs in materials of varied albedo ranging from very low to very high. These layers are well exposed in several small hills and also appear, although more subtly, in flatter regions of the ellipse (Figure 7). The upper layers are without doubt stratigraphically connected with Ma'adim's most recent flow, as indicated by the direction of the layering. However, for all layers located below the most superficial levels, it is impossible to conclude that they are necessarily from the same source. The difference in albedo could be either an indication of materials from various sources that could be detected by THEMIS or represent different levels of weathering and alteration of the same type of material. For instance, extremely bright albedo patches in the central region of the ellipse could either be ash from volcanic events, playas and evaporites from lacustrine episodes, or aeolian and/or global air fall deposits from material whose source could be located far from Gusev or Ma'adim.

[26] The MOLA altimetric profiles and MOC images seem to be consistent with the hypothesis of a lake in Gusev, although other interpretations are possible. The elevation of the most recent floor of Ma'adim Vallis is concordant with Gusev's floor. The MOLA profiles of Ma'adim's floor are altimetrically concordant with the MOLA profiles of the topset of the mesas located at the outlet of the channel as expected in a deltaic setting. The elevation of the first terrace of Ma'adim is concordant with the proposed delta's topset (Figure 8). The morphology of the mesas also is consistent with a Gilbert-type delta and formation in a sublacustrine environment [*Grin and Cabrol*,

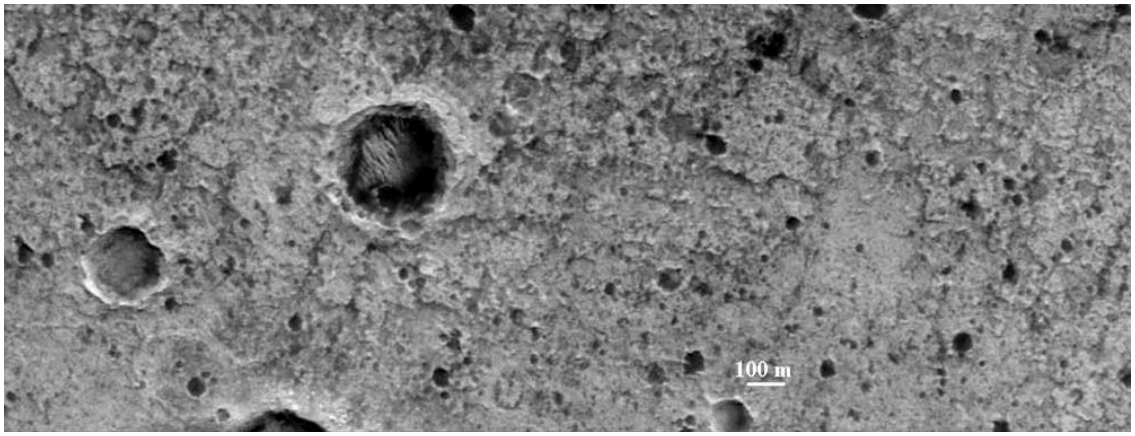

Figure 7. Spectacular image of an eroded impact crater. This type of crater is well represented in the eastern region of the landing ellipse (south of Thyra). Many layers are exposed in what could be an ancient ejecta deposit, which are likely to have brought to the surface the record of many geological and climatic episodes. It is likely that a large variety of mineralogies and materials originating from diverse processes and epochs are exposed at these sites. (MOC image E05-00471 centered at 15°09′S and 184°42′W (3.44 m/pixel) resolution.) Courtesy of NASA/JPL/Malin Space Science Systems.

1997]. This landform is currently the largest presumed deltaic structure identified on Mars. From image and altimetry analysis, aeolian processes alone could not had produced such concordance. However, aeolian processes have been prominent in modern times on Mars and are shaping the landscape of Gusev in a spectacular fashion by exhuming rocks and sedimentary materials in some places and forming dunes in others.

3.4. Wind Features

[27] The floor of Gusev crater exhibits a variety of wind-related features, including dune forms, albedo patterns, and features that could have formed by wind erosion [*Greeley et al.*, 2003]. Most of the dune forms occur on the floors of small impact craters (which apparently served as ''traps''), while others exhibit morphologies typical of barchan dunes with ''horns'' indicating the prevailing direction of the wind at the time of their formation [*Breed et al.*, 1997]. Dunes are considered to be composed of sand-sized particles (~60–2000 μm in diameter), derived locally [*Greeley et al.*, 1992].

[28] Albedo patterns that are considered to be related to winds include a large dark swath that cuts across the floor of Gusev more than 100 km from the mouth of Ma'adim Vallis. This albedo pattern is well seen on Viking Orbiter images taken in the late 1970s, but shows changes in images taken by subsequent spacecraft, including Phobos 2, MGS, and MO. The primary change is a brightening in the middle of the pattern. Smaller albedo features include both bright and dark streaks associated with small craters. The orientations of these features are considered to represent the direction of formative winds.

[29] Parts of the floor of Gusev Crater include small (few hundred meters across) knobs that tend to be elongated in the direction of the wind. These features could represent wind erosion, although some of the elongation could be due to accumulation of windblown materials in the immediate lee of the hills.

[30] *Greeley et al.* [2003] mapped the orientations of the various wind related features and compared them with atmospheric model predictions of global-scale and regional-scale winds. Results show that the features correlate with strong, global-scale seasonal winds from the southeast, and as a function of time of day. The diurnal winds are particularly important as they relate to topography, with winds flowing into the crater at nighttime and winds flowing radially out of the crater as heating builds through the day and into the afternoon. These winds flow ''upstream'' at the mouth of Ma'adim Vallis and appear to be responsible for the formation and orientation of the barchan dunes in this area [*Fryberger et al.*, 1979].

[31] MER has the potential to address several aspects of the aeolian regime within Gusev Crater. Although there is no instrument to measure the wind speed and direction, images will enable the identification and mapping of wind-related features within the operations area of MER. Orientations of features such as dunes, ventifacts, and wind streaks associated with rocks will enable determination of wind directions at the time of their formation. Although only the large dark zone on the crater floor is known to have changed since the Viking mission, it is possible that at least some aeolian features would be active during the MER mission. For example, plans are being made to observe possible accumulation and removal of dust from surfaces on the rover deck. Concurrent observations of the MER site from orbit through the Odyssey and Mars Express missions could provide insight into the aeolian regime within and around the crater for correlation with observations from the ground. Trenches dug by MER in drift deposits and estimates of the physical properties of the sediments will provide insight into the nature of windblown materials.

3.5. Impact Crater Hydrothermal Deposits

[32] Impact-generated hydrothermal systems and associated deposits have been identified as important targets in the

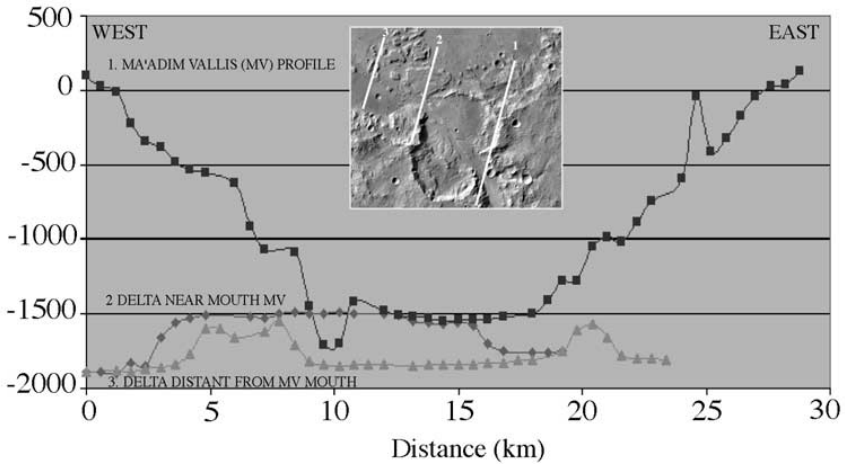

Figure 8. Comparison of three MOLA altimetric profiles in Ma'adim Vallis to test the fluvio-lacustrine hypothesis. Profile 1 is mainly crossing the higher section of the valley and the upper terraces. The smaller section in that profile corresponds to the youngest channel. When compared to the highest elevation of profile 2, which mostly covers what was suggested to be a deltaic mesas, continuity in elevation is obvious between the elevation of Ma'adim higher terraces and the suggested deltaic mesa. This observation is consistent with fluvio-deltaic dynamics. Profile 3 (at the left border of the figure) shows the lowering in elevation of the mesas as the deposition happened farther away toward the center of the basin. Courtesy of NASA/JPL/Malin Space Science Systems.

search for ancient habitable environments on Mars and a preserved record of prebiotic chemistry, or fossil biosignatures [*Farmer and Des Marais*, 1999; *Hagerty and Newsom*, 2001; *Newsom et al.*, 2001]. These comprise primary objectives of the MER mission. In large craters the nature and geometry of the heat sources and the zones of higher permeability control the location of hydrothermal deposits. The heat sources are the impact melt sheet on the crater floor, and the uplifted basement [*Newsom*, 1980; *McCarville and Crossey*, 1996; *Thorsos et al.*, 2001]. Recent results by *Thorsos et al.* [2001] indicate that these two sources of heat were approximately equal during the formation of large craters in the southern highlands. Studies of terrestrial hydrothermal systems and theoretical studies of Martian systems by *Gulick* [1998] and *Rathbun and Squyres* [2002] show that focusing of hydrothermal fluids occurs at the edge of planar heat sources. Both geological evidence and modeling suggest that the flow of hydrothermal fluids in craters will be concentrated at the edges of the melt sheets in zones of higher permeability in the crater rim and central uplift, where hydrothermal deposits are expected [*Gutmann*, 2002].

[33] The hydrothermal potential for craters can be estimated from the total heat available from impact melt and uplift. Gusev crater, 150 km in diameter, may have as much as 10,000 km^3 of impact melt, corresponding to a layer 500 m thick. The total heat available in this crater, assuming equal amounts from uplift and impact melt is 1.4×10^{23} Joules. For comparison, this amount of energy is 56 times the amount of heat released at Yellowstone over a 15,000 year period (2.5×10^{21} joules) [*Fournier*, 1989]. However, the Gusev landing site ellipse is apparently covered with deposits of diverse origins, making access to the underlying melt sheets very unlikely. The most likely source of hydrothermal deposits in the Gusev landing site is from the 20 km diameter rim of Thyra Crater, which surrounds the northeast portion of the landing ellipse (Figure 9). Although orders of magnitude smaller than Gusev itself, Thyra's formation may have resulted in the formation of 10 km^3 of impact melt, and a substantial hydrothermal system. An important question is whether Thyra also excavated the underlying impact melt sheet in Gusev or deposits within the basin. On the basis of the normal depth of excavation in large craters of about 10% of the crater diameter [*Melosh*, 1989] Thyra is very unlikely to have excavated the impact melts, but excavation of deposits that followed is likely. Because the ejecta from Thyra appears to be buried, only later impacts and possibly fluvial transport from the rim of Thyra might have delivered impact melts onto the lake deposits.

[34] Hydrothermally altered material and deposits from the rim and floor of Gusev also may have been transported to the landing site by the formation of superimposed craters. We have identified several craters on the rim of Gusev that could have delivered material to the ellipse in the form of ejecta (Table 1). Most of this material is undoubtedly buried, although some could have been reexcavated by the formation of Thyra. Craters G6 and G7 (see Figure 9) are apparently the youngest that could have supplied material to the ellipse, but they are quite far from the center of the ellipse where the mission has the greater probability to land. G7 could have delivered hydrothermal deposits from G5 and the rim of Gusev to the landing ellipse. Alternative mechanisms for delivering material to the floor of Gusev include fluvial transport (e.g., G2, G3) as well as mass wasting of the crater rim, which could contribute material from crater G5 to the southwest portion of the ellipse. Higher-resolution imaging of the rim of Gusev including THEMIS data [see *Christensen et al.*, 2003] may help

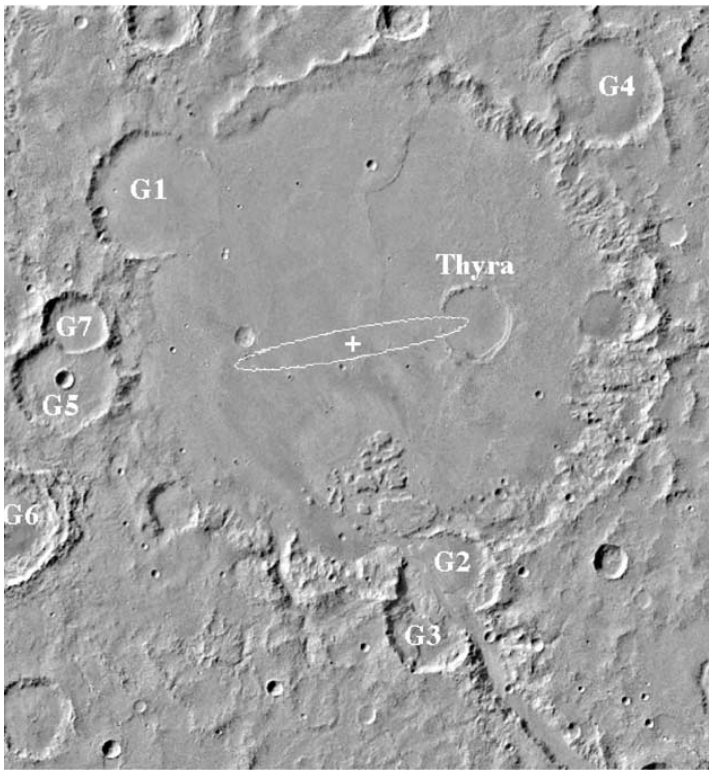

Figure 9. Locations of superimposed impact craters surrounding the landing site ellipse in Gusev. Hydrothermally altered impact melt and basement material from the rim of Gusev may have been transported to the ellipse as ejecta during formation of the superimposed craters or by fluvial processes. In some cases, such as Thyra, hydrothermal materials produced during the cooling of the superimposed craters may be present in the ellipse. The length of the ellipse is 90 km.

establish the relative ages of the ejecta blankets of the superimposed craters and the surficial materials in the landing site ellipse.

4. Testable Hypotheses for MER

[35] Spirit's suite of sensors and imaging systems are anticipated to provide insight into the depositional and soil formation processes that have occurred in Gusev Crater [*Squyres et al.*, 2003]. Integrated observations that will be key for assessing the nature of past and present geological processes and environments include geochemistry, mineralogy and microtextural information obtained from rocks and soils. While lacustrine processes may have supplied significant material to Gusev, volcanic, fluvial [*Kuzmin et al.*, 2000], aeolian [*Greeley et al.*, 2003], and glacial processes [*Grin and Cabrol*, 1997] are likely to have contributed material too. The basic rock and soil characteristics that may

Table 1. Impact Craters Contributing Material to the Landing Ellipse

	Gusev Crater Landing Site Name or Identification Number								
	Gusev	Thyra	G1	G2	G3	G4	G5	G6	G7
Crater diameter, km	150	21	37.9	32.7	26.6	32.7	31.1	33.8	19
Distance from center to ellipse center, km		28.5	86.9	65.2	76.9	103.9	91.8	118.6	80
Distance from center to ellipse center (crater diameter), km		1.36	2.29	2	2.89	3.18	2.95	3.51	4.21
Distance from crater edge to ellipse center, km		18	67.9	48.9	63.6	87.6	76.3	101.7	70.5
Distance from crater edge to ellipse center (crater diameter), km		0.86	1.79	1.5	2.39	2.68	2.45	3.01	3.71
Latitude, deg		−14.64	−14	−15.93	−16.15	−13.47	−14.93	−15.65	−14.4
Longitude, °W		184.34	186.01	184.44	184.52	183.68	186.44	186.75	186.4
Melt volume, km^3	10,300	12	124	75	32	75	75	75	10
Heat of Yellowstone equivalents	57	0.1	0.5	0.3	0.2	0.3	0.3	0.3	0.1

Table 2. Main and Subhypotheses on the Origin of the Sediments and Material in Gusev Landing Ellipse[a]

Main Hypotheses for Sediments Origin	Subhypotheses	Origin
1. Lacustrine	1.1. perennial lake	1.1.1/1.2.1. precipitation
	1.2. episodic lake	1.1.2/1.2.2. groundwater
		1.1.3/1.2.3. hydrothermal water
		1.1.4/1.2.4. glacial meltwater
		1.1.5/1.2.5. combination of two or more of the above sources due to changing conditions through time
2. Fluvial	2.1. runoff	2.1.1/2.2.1. precipitation
	2.2. outflow from intravalley lake	2.1.2/2.2.2. groundwater
		2.1.3/2.2.3. hydrothermal water
		2.1.4/2.2.4. glacial meltwater
		2.1.5/2.2.5. combination of two or more of the above sources due to changing conditions through time
3. Glacial	3.1. glacier	3.1.1. local snow and ice packs
		3.1.2. regional glaciation
	3.2. ice-covered stream	3.2.1. free water underneath the ice until the water supply ceased
		3.2.2. progressive complete freezing down of the water
4. Volcanic	4.1. plastic flow[b]	4.1.1. hyperfluid lava
		4.1.2. viscuous lava
		4.1.3. pyroclasts and ashes are filling Gusev basin
5. "Exotic" fluid	5.1. CO_2 flow[c]	5.1.1. liquid CO_2 reservoir
	5.2. clathrate flow[c]	5.2.1. clathrate reservoir
6. Aeolian	6.1. regional to local winds[d]	6.1.1. wind regimes
	6.2. global air fall[e]	6.2.1. global atmosphere circulation.
7. Subsurface hydrothermal	7.1. hydrothermal minerals	7.1.1. impact-generated
		7.1.2. crustal magma sources

[a]The subhypotheses shown reflect discussions about processes that have been presented in the literature over the years, either for the formation of the Ma'adim Vallis/Gusev crater system or for channels in general on Mars.
[b]Hyperfluid lava carved Ma'adim Vallis and deposited material in Gusev. Viscuous lava generated a landform that mimics a delta at the outlet of Ma'adim. Pyroclasts and ashes are filling Gusev basin.
[c]Obliquity changes provided temperature conditions for CO_2 or clathrates release at the latitude of Ma'adim and Gusev. The surface pressure is still problematic.
[d]Wind regimes following climate changes have driven the deposition and exhumation of material in Gusev.
[e]Sediments in Gusev are made of material extracted over the planet and deposited in the basin by global atmosphere circulation.

be addressed with the Athena instrument payload in testing the various depositional hypotheses are reviewed in the following section.

4.1. Main Hypotheses

[36] Data from the Viking, MGS, and MO missions have allowed several main hypotheses (Table 2) to emerge that attempt to explain the spectral and albedo characteristics of surface material and the geomorphology observed in Gusev. Each main hypothesis carries a set of subhypotheses that require in situ measurements for either accepting or rejecting the subhypotheses. The variations of each subhypotheses are not mutually exclusive and in some cases overlap each other.

4.2. Soil Formation and Sedimentary Processes

[37] The main hypotheses can be associated with specific soil and/or sediment types that may be detected by the Athena instrument payload which include: (1) global soil; (2) soils formed in a nonaqueous environment; (3) soils formed in an aqueous environment; (4) volcanic materials; (5) lacustrine sediments; (6) fluvial sediments; (7) aeolian sediments; and (8) glacial sediments. Soil and sediment profiles may be observed in the form of ejecta blocks from impact events, outcrops, and aeolian exposures (e.g., yardangs, see Figure 10). Excavation by spinning a rover wheel while the rover remains stationary is also anticipated to access soil and sediment 5–10 cm below the surface.

[38] This discussion cannot touch on all possible signatures of all sediment and soil formation processes that could be detected by the Athena instruments. Moreover, we do not presume to have identified every possible type of soil or sediment that could conceivably occur within Gusev. This is meant as a guide, and attempts to demonstrate what the Athena instruments may detect and what hypotheses could be identified if presented with certain evidence of a geologic or pedogenic process. Table 3 summarizes what results from the Athena instruments would suggest a particular geologic or pedogenic process listed above and is supported by the following discussion.

4.2.1. Global Soil

[39] The Viking and Mars Pathfinder (MPF) sites show widely similar bulk soil elemental compositions, suggesting a soil that has been globally distributed by aeolian activity [*Rieder et al.*, 1997]. The presence of global soil in Gusev will be indicated by alpha particle X-ray spectrometer (APXS) bulk chemical analyses reporting elemental concentrations similar to the Viking and MPF sites. Further support for global soil in Gusev may be established if Pancam multispectral imaging shows spectra similar to what was obtained by MPF [*Bell et al.*, 2000].

4.2.2. Soil Formation in a Nonaqueous Environment

[40] The APXS data of soils derived from local rocks will be expected to have total elemental composition similar to the local rock. Furthermore, Mini-TES and Mössbauer spectrometer (MB) spectra would show that the rocks and soils have similar spectral properties. Soils that show no evidence of secondary mineralogy (e.g., clay minerals, iron-oxyhydroxides, carbonates, and sulfates) would suggest that the soils were not affected by postdepositional aqueous

Figure 10. Yardangs of lake bed deposits in the Farafra depression, Egypt. The height of the dome is about 10 m. Reproduced with permission from John Wiley & Sons Limited [*Breed et al.*, 1997].

activity. The Microscopic Imager (MI) data may show soil particles with angular morphology suggesting that they were derived locally.

4.2.3. Volcanic Ash/Maar Base Surge Deposits

[41] Apollinaris Patera is 250 km north [*Robinson et al.*, 1993] and may have deposited volcanic ash and pyroclasts in Gusev [*Kuzmin et al.*, 2000]. The detection of blocky, platy, and/or cupsate glass shards by MI will support the idea that volcanic ash is component of the soil [*Orton*, 1996]. Mini-TES spectra of an ash deposit may show a basaltic or andesitic signature if the ash has significant lithic component. Ash deposits with a significant vitric component would tend to show a poorly crystalline Mini-TES spectra. If the volcanic ash is not altered by water, the MB may detect Fe phases such as ilmenite, titanomagnetite, titanomaghemite, and magnetite and Fe containing pyroxene [*Fischer and Schmincke*, 1984; *Gunnlaugsson et al.*, 2002].

[42] While craters in Gusev are presumed to be of impact origin, it is conceivable that some craters could be maars or tuff rings (Figure 11). Maar or tuff ring volcanoes can produce base surge deposits that resemble fluvial deposits (e.g., planar to wavy layering) as shown in Figure 12. However, unlike fluvial deposits, base surge deposits may contain soft sediment deformations (i.e., folded layering between undeformed layer), vesicles (gas bubbles) and bedding sags that may be observable with Pancam [*Cas and Wright*, 1987; *Fischer and Schmincke*, 1984].

4.2.4. Soil Formation in Aqueous Environment

[43] The observation of platy, blocky, prismatic, and/or columnar, soil structures in an exposed soil profile by the Pancam would suggest that the soil may have been affected by water. Extensive leeching of base cations from the soil profile would have occurred regardless of whether Mars had a reducing or an oxidizing environment. Soil levels of Ca, Mg, K, and Na as detected by the APXS may be lower relative to local rocks. Mini-TES may detect clay minerals (e.g., kaolinite, vermiculite, chlorite, and smectite), gibbsite, Fe-oxyhydroxides [e.g., ferrihydrite ($5Fe_2O_3 \cdot 9H_2O$), goethite (FeOOH), or hematite (Fe_2O_3)], and calcite ($CaCO_3$). MB could detect the presence of any Fe-oxyhydroxides.

[44] Arid soils experiencing low or episodic water activity can develop structure as discussed above. Vesicular porosity is prevalent near the soil surface in arid soils [*Dunkerley and Brown*, 1997] and may be observable by the Pancam and MI. Arid aqueous activity would be indicated by the APXS detecting elevated levels of Ca, Mg, K, Na, S, Cl, and/or N in the soil relative to local rock. Mini-TES may detect calcite ($CaCO_3$), gypsum ($CaSO_4 \cdot 2H_2O$), annhydrite ($CaSO_4$), and possibly nitratite ($NaNO_3$) [*Eriksen*, 1981; *Clark et al.*, 1982; *Amit and Yaalon*, 1996; *Li et al.*, 1996; *Böhlke et al.*, 1997]. Smectite is usually the prevalent clay mineral formed in arid environments [*Allen and Hajek*, 1992] and could be detected by Mini-TES.

[45] The above discussion of aqueous weathering assumed Earth oxidizing conditions. Reducing conditions could well have prevailed during aqueous mineral weathering on early Mars [*Catling*, 1999]. Siderite ($FeCO_3$) may have formed in greater abundance than calcite [*Catling*, 1999]. Under reducing conditions magnetite (Fe_3O_4), siderite, and pyrite (FeS_2) would have the potential to precipitate rather than goethite, ferrihydrite, or hematite. The prevalence of the apparent oxidizing conditions on Mars today may obscure any evidence of reducing mineralogy. The abrasion of a sedimentary rock or indurated soil blocks with the RAT to analyze material not directly exposed to the past and/or present Martian oxidizing conditions should allow MB and Mini-TES to test the existence of reducing mineralogy.

4.2.5. Lacustrine Sediments

[46] Pancam could detect soil profiles of a lake deposit showing alternating layers of light colored salts and darker colored clay/silt layers [*Li et al.*, 1996]. However, complex mixtures of evaporites and clay mineralogies can occur in lacustrine soils and may not be discernable by Pancam. Soil structure in lacustrine soils may also be observable by the Pancam. Evaporite and clay minerals may also be detected by Mini-TES. The APXS may show elevated levels of Ca, Mg, K, Na, S, Cl and possible N relative to local rock. Pancam and MI could detect a lake's margin because of the presence of beach sands and gravels relative to clays and silts that occur toward the center of the lake. Some of the

Table 3. Possible Results From Athena Instruments of Hypothetical Soils and Sediments in Gusev Crater[a]

Hypothesis	Panoramic Camera	Microscopic Imager	Alpha Particle X Ray Spectrometer	Mini-Thermal Emission Spectrometer	Mössbauer Spectrometer
Global soil	**Similar multispectral characteristics as MPF soil.**	No uniquely identifiable characteristics.	**Similar elemental chemistry as MPF and VL 1, 2 soil.**	No uniquely identifiable characteristics.	No uniquely identifiable characteristics.
Soils from physical weathering of local rock	No uniquely identifiable characteristics.	Angular soil grain morphology.	Soil elemental chemistry similar to local rock chemistry.	Soil spectra similar to local rock spectra. No secondary mineralogy.	Soil Fe mineralogy similar to local rock Fe mineralogy. No secondary Fe-oxyhydroxides.
Volcanic ash	Sedimentary deposit that conforms to topography.	Glass shards cupsate, blocky, platy <250 μm.	Any range of Si content. Chemistry may be different than local rock.	Poorly crystalline to crystalline material (e.g., plagioclase, pyroxene, hornblende).	Ilmenite, titanomagnetite, titanomaghemite, magnetite, Fe-pyroxene.
Maar base surge deposit	Massive, planar sedimentary deposits. **Soft sediment deformations, vesicles, bedding sags.**	Glass shards, blocky. Fine-grained material <1 mm.	Any range of Si content.	Poorly crystalline to crystalline material (e.g., plagioclase, pyroxene, hornblende).	Ilmenite, titanomagnetite, titanomaghemite, magnetite, Fe-pyroxene.
Soil from aqueous weathering (e.g., melting snow)	**Soil structure. Columns, wedge, blocky, platy. Vesicular porosity near soil surface.**	**Vesicular porosity near soil surface.**	Loss or accumulation of Ca, Mg, K, Na relative to local surface rock.	Phyllosilicates, carbonates, sulfates, secondary Fe-oxyhydroxides.	Secondary Fe-oxyhydroxides.
Fluvial deposit	**Conglomerate facies;** sheet, tabular cross stratified, lateral, channel fill, **rounded/subrounded clasts up to 30 cm.**	No visible grains.	No uniquely identifiable characteristics.	Primary minerals with cementing mineralogy; Fe-oxyhydroxide, carbonate, or phyllosilicates.	Detect mineralogy of Fe-cementing mineral if present. Possible siderite ($FeCO_3$) Fe^{2+}-smectite if outer oxidized layer on sedimentary rock is removed by the RAT.
	Sandstone facies; tabular and trough cross bed and ripple bed.				
	Shale facies; planar bed.				
Lacustrine deposit	Alternating planar layers of light-colored layers with darker layers. Layer thickness few cm to 10s cm.	Sand and gravel grains at lake's margin; clay/silt grains toward lake's center.	High levels of Ca, Mg, K, Na, S, Cl, N in basin.	Mineralogy variation from lake margin to lake center (e.g., carbonate → sulfate); phyllosilicates.	Possible siderite ($FeCO_3$) Fe^{2+}-smectite if outer oxidized layer on sedimentary rock is removed by the RAT.
	Lake's margin: sandstone facies; possibly similar to fluvial facies.	Rounded sand grains.			
	Lake's middle: shale facies; planar layers of silt/clay.	No visible grains.			
Aeolian deposit	No particles larger than can be moved by creeping.	Grain size <4 mm.	Sediment chemistry differing from local rock chemistry.	Comparisons of sediment and local rock spectra suggest differing mineralogies.	Comparisons of sediment and local rock Mössbauer spectra suggest differing Fe mineralogies.
	Sandstone facies: planar, laminar cross bedding or ripple bedding. No trough cross bedding.				
	Presence of global soil (see above).				
	>**20 m thick deposits with little stratification (loess).**	Grain size not easily discernable (loess).			

Table 3. (continued)

Hypothesis	Panoramic Camera	Microscopic Imager	Alpha Particle X Ray Spectrometer	Mini-Thermal Emission Spectrometer	Mössbauer Spectrometer
Glacial deposit (glacial till/moraine)	**Poorly sorted material; cm to large boulders, striated rocks, gravel, boulders. Flattened rocks and gravel.**	**Striated rocks and gravels.**	No uniquely identifiable characteristics.	Primary minerals.	Primary Fe minerals.
Glacial lake	**Varves, rain-out debris in planar layered sediments.**	No visible grains.	High levels of Ca, Mg, K, Na, S, Cl, N	Phyllosicates.	Possible siderite ($FeCO_3$) Fe^{2+}-smectite if outer oxidized layer on sedimentary rock is removed by the RAT.

[a]Bold text of instrument analytical results suggest a positive identification of an individual hypothesis.

precipitation sequence of (carbonates → sulfate) → halite could be detected as Mini-TES and APXS sample from the outer reaches of the lake and moves toward the center of the lake [*Eugster and Kelts*, 1983; *Shaw and Thomas*, 1997]. Within a 600 m traverse, the spectrometers and cameras onboard the rover are likely to observe chemical transition. Soils with abundant evaporite minerals could be indurated, and clay mineral deposits may become shale-like. Any shale-like material with planer layering or indurated evaporites may occur as ejecta blocks large enough to be examined with the Athena instruments.

4.2.6. Fluvial Sediments

[47] Evidence of past fluvial activity in Gusev crater may occur as ejecta blocks or outcrops of conglomerate, sandstone, or shale at the surface. Any material exhibiting layered morphology (e.g., cross bedding, ripple bedding and trough cross bedding) [*Collinson*, 1996] observed by Pancam are candidates for fluvial deposition. Rounded soil grains observed by MI would suggest fluvial activity. Mini-TES would detect the primary mineralogy of the sand or conglomerate particles and may detect their cementing agents (e.g., silica, carbonate, clay, iron oxyhydroxides) [*Klein and Hurlbut*, 1993]. The color of the sandstone may reflect the cementing agent with silica and carbonate agents producing a light color and the iron oxyhydroxides producing a red to reddish brown color. If an iron-oxyhydroxide or siderite is the primary cementing agent, then MB may indicate the iron mineralogy of the cementing agent. PanCam images of a rock or outcrop material showing planar layering with no MI identifiable sand-sized grains would suggest shale-like material. Mini-TES would produce spectra with primary mineralogies and clay mineralogies. Shale-like material containing a significant vitric component derived from volcanic ash would tend to produce poorly crystalline Mini-TES spectra.

4.2.7. Aeolian Sediments

[48] Detection of the global soil would suggest aeolian deposition of soil. MI will detect aeolian sedimentary deposits that show planar cross bedding and rippled bedding if the aeolian grains are large (>30 μm. However, trough cross bedding that occurs in fluvial environments typically does not occur in aeolian environments. Furthermore, layering of materials coarser than 4mm would suggest only fluvial and not aeolian activity [*Greeley et al.*, 1992].

[49] Loess deposits on Earth tend to be 20–30 m thick but have been known to be as thick as 60 m and usually are derived from fluvial and glacial sediments [*Pye*, 1987; *Dunkerley and Brown*, 1997]. Loess particle sizes range from 10 to 50 μm and are usually deposited in weakly stratified accumulations. Any Pancam and MI observations of deposits that appear to have little or no stratification with particle sizes barely or not visible by the MI may indicate loess.

4.2.8. Glacial Sediments

[50] Soil profiles or outcrops containing glacial till or material deposited at the terminus (moraine material) of a glacier will be poorly sorted and contain all grain sizes ranging from clay-sized grains to meter-sized boulders. The layering observed with glacially deposited material could look similar to fluvial material. However, closer examination of rock fragments (>2 mm) in glacial till could show indications of striations resulting from the abrasion of the rock, which is characteristic of the grinding action of glaciers

Figure 11. Remnant of the maar volcano, Crater Elegnate in the Pinacate volcanic field, Sonora, Mexico. The diameter of the crater is about 5 km. Reprinted from *Gutmann* [2002], with permission from Elsevier.

on rock against another rock or bedrock surface. Some striated pebbles or rock may be elongated or flattened and would lie in the direction of glacial movement. "Rain-out" debris from rafted ice that is deposited in the lake's sediment may indicate a glacial lake [*Bennett and Glasser*, 1996]. Varves are usually indicative of glacial activity and, if so, consist of alternating layers of clay and silt/sand in the lake's sediment. Varving also occurs in temperate climates with seasonal fluctuation in precipitation. All of the above indicators of glacial activity may be observed with Pancam or MI.

[51] It is important to note that the key indicators for each of the described hypotheses could all be identified in situ within the range of the rover traverse as they are strongly based on the mineralogy of sedimentary exposures and grains and their morphology. In situ observations from the rover will be then complemented by larger-scale orbital data surveys (MGS and MO) during the mission in order to fully understand the significance of the observation and the results of the measurements.

5. Gusev and the Habitability Potential of Mars

[52] The terrestrial fossil record of microbial life encompasses a wide range of mesoscale biosedimentary structures (centimeter scale to meter scale), microscale biofabrics (millimeter scale), cellular structures (micron scale) and associated biogeochemical signatures. Studies of the processes of microbial fossilization in modern terrestrial environments are considered good analogs for the early Earth and Mars and have revealed patterns that are consistent with the Precambrian fossil record [*Farmer and Des Marais*, 1999]. This has allowed the identification of factors important in determining the long-term preservation potential of microbial biosignatures. Important factors include: (1) intrinsic properties of the organisms (e.g., the presence of recalcitrant cellular of extracellular structures) and (2) extrinsic environmental factors, such as the redox environment and the chemical stability of the entombing minerals during diagenesis. While it is challenging to speculate about the nature of intrinsic factors that might have influenced a putative Martian fossil biota, MER has tools useful for the assessment of the extrinsic factors of past Martian environments important for assessing preservation potential.

[53] Terrestrial studies have shown that the long-term preservation of microbial biosignatures is most favored

Figure 12. Planar layers of a base surge deposit from the Quill, St. Eustatius, Lesser Antilles [from *Cas and Wright*, 1987]. The height of the figure is about 2 m.

when microorganisms, or their by-products are rapidly entombed by fine-grained detrital sediments, or chemical precipitates of stable mineralogy and low permeability. Such factors conspire to create a closed chemical system that protects against the loss of organic materials and microtextural information during diagenesis. Chemical sediments composed of silica, phosphate, and carbonate minerals, and fine-grained, clay-rich detrital sediments, or water-deposited volcanic ash are examples of lithologies that are favorable for long-term preservation. In fact, most of the microbial fossil record on Earth is preserved in such lithologies. These extrinsic factors of preservation are based on basic physical and chemical laws that would appear to have universal application. Hence they play a central role in Martian exopaleontology and are the prevailing strategies for exploration of a Martian fossil record [*Farmer*, 2000a, 2000b].

[54] Terminal lake basins, such as that postulated for the Gusev Crater, provide especially favorable depositional settings for capturing and preserving fossil biosignatures [*Farmer and Des Marais*, 1999, and references therein]. Such paleoenvironments have high potential for having accumulated fine-grained, clay-rich sediments and/or water-lain volcanic ash deposits in deeper basin areas and/or chemical precipitates (e.g., evaporates) along shallow basin margins, or on basin floor playas. In addition to the high preservation potential of these low-temperature aqueous sedimentary deposits, the precipitates of hydrothermal systems have also been shown to be important repositories for a variety of microbial biosignatures [*Farmer*, 2000a, 2000b]. Large impact structures like Gusev are expected to have generated melt sheets and central uplifts capable of driving prolonged hydrothermal systems [*Newsom et al.*, 2001]. Such systems typically leave behind a variety of surface and subsurface mineral deposits [*Farmer*, 1996; *Hofmann and Farmer*, 2000] that could have been later recycled and deposited as detrital sediments on the Gusev Crater floor.

[55] The MER rovers will each be equipped with high-resolution visible range wavelength cameras (PanCam), a mid-IR spectrometer (Mini-Thermal Emission Spectrometer) and a variety of contact sensors for determining the geochemistry (Alpha Proton X-ray Spectrometer), mineralogy (Moessbauer spectrometer) and microstructure of rocks and soils (Microscopic Imager). In addition, the Rock Abrasion Tool (RAT) will provide access to fresh rock interiors. Collectively, these instruments will provide a powerful analytical package for assessing the composition and microstructure of surface materials. This will mark the first step toward an in situ evaluation of the nature of paleoenvironments, their potential habitability and preservation potential.

[56] However, MER also has the potential to detect biosignatures within rocks over a range of spatial scales. Studies of microbial fossilization processes in terrestrial environments that are considered good analogs for the early Earth and Mars have shown that mesoscale biosedimentary structures (e.g., stromatolites of other biolaminated sediments) and their associated microstructures tend to be favored in long-term preservation over cellular-scale structures [*Farmer*, 1999]. PanCam and MI will provide observations over the range of spatial scales typically observed for these types of terrestrial features. However, taken alone, such mesoscale and microscale structures can present an interpretive challenge as they are often undiagnostic with regard to biogenicity.

[57] The degradation of cellular materials typically produces a variety of stable organic compounds and kerogen that is often abundantly preserved in fine-grained (low permeability), clay-rich detrital sediments (shales) and water-laid volcanic ash deposits. The detection of carbon-bearing compounds within suspected laminated sediments of this nature could be highly suggestive of a biological origin. This indicates the importance of combining observations from all of the MER instruments to adequately constrain interpretations and to test hypotheses, whether for assessing paleoenvironmental conditions and potential habitability, the preservation potential, or suspect fossil biosignatures.

6. Conclusion

[58] Gusev Crater is a site that has the potential to address the science objectives of the MER missions. These questions and the ways in which investigations in Gusev can address them are summarized here.

[59] 1. As concerns the question of water, among the main hypotheses, fluvial and lacustrine have a leading role with the input of the new MGS and MO data. Gusev shows evidence consistent with the role of past water, fluvial and lacustrine activity, and the concentration of a flow in a basin. If the fluid that carved Ma'adim and deposited sediments in Gusev is not water but an ''exotic'' fluid such as CO_2 [*Hoffman*, 2000] or clathrates, it would make the landing in Gusev equally critical. Ponding of such a fluid for extended periods of time in a basin would provide a unique opportunity to discover its composition, chemistry, and the associated sedimentation processes and mineralogy. As the morphologies created by such flow strongly mimics those of fluvio-lacustrine processes, it would be essential to understand what has biased our interpretation for so many years and what it implies for other channels, valleys, ponds and lakes on Mars. It could be a complete revolution in our perception of the Martian environment and its possibility as an abode of life.

[60] 2. As concerns the question of geological history, basins are notorious for collecting the record of climatic changes. Whether the materials in Gusev are aqueous, glacial, lacustrine, volcanic, aeolian, ''exotic,'' or all of the above, the basin has maintained a record of the conditions under which these material have been deposited and formed. MOC has clearly shown that the central hills and other exposures on the floor of Gusev are layered. Laminations and possibly rhythmites and varves located near the center of the ellipse hold the keys to the geological diversity of Mars. As no hypotheses exclude the other, we might have aqueous, lacustrine, volcanic, impact, and aeolian material exposed in accessible layers at the landing site

[61] 3. As concerns the question of climate, the same layers, together with the morphology of the deposits and, the microscopic study of the sedimentary grains and their mineralogy will provide indicators to infer climatic conditions. For instance, convoluted varves will indicate that a body of ice was resting and putting pressure on the sediments. Minerals that form in specific temperatures and pressures ranges could also be an indication of climatic

conditions. By gathering converging evidence, plausible climate conditions might be inferred.

[62] 4. As concerns the question of life, finding fossils is a difficult endeavor even on Earth unless they are extremely abundant and/or one knows well the geological formations and their succession. This is not yet the case on Mars. The primary role of MER will be to explore an ancient environment that could have been suitable for life. In short, it will test the habitability potential of Mars at the two landing sites. If the fluvio-lacustrine hypothesis is confirmed, Gusev Crater is probably one of the most favorable places on Mars to land and test the habitability hypothesis. It shows evidence consistent with a long-term fluvio-lacustrine history in a confined basin. Such conditions usually favor chemical and biological processes, at least in terrestrial analog environments. As noted earlier, fossilization processes are especially favored in such terminal lacustrine settings. The landing ellipse, and its central region in particular, are located at the distal end and deepest point of the proposed paleolake. This central location is optimal in exploring for deep basin shales or volcanic ash deposits that could harbor a fossil record [*Farmer*, 1995]. The mobility of MER will be a critical element as such an investigation requires coverage of large amount of ground area in order to increase the statistical chance of finding evidence of biological processes.

[63] Gusev Crater also is an excellent site from an education and public outreach perspective. Students and the general public will be drawn to the visual accessibility of the site. Previous Mars lander missions have never explored a place similar to Gusev Crater. Coupling the novelty of the site with the ease of explaining how it fits within NASA's Mars exploration goals to a nontechnical multi-aged audience gives Gusev extraordinary potential to capture the public's imagination. The exploration of Gusev Crater can be used to infuse excitement into lessons on geology, biology, astronomy/space science, and environmental science taught in precollege classrooms across the globe, and to inspire the next generation of scientists and engineers.

[64] **Acknowledgments.** The authors thank the two anonymous reviewers for their constructive comments.

References

Allen, B. L., and B. F. Hajek, Mineral occurrence in soil environments, in *Minerals in Soil Environments*, edited by J. B. Dixon and S. B. Weed, pp. 199–278, Soil. Sci. Soc. of Am., Madison, Wis., 1992.

Amit, R., and D. H. Yaalon, The micromorphology of gypsum and halite in Reg soils—The Negev Desert, Israel, *Earth Surf. Processes Landforms*, *21*, 1127–1143, 1996.

Arvidson, R. E., M. Coradini, A. Carusi, A. Coradini, M. Fulghignoni, C. Federico, R. Funiciello, and M. Salomone, Latitudinal variation of wind erosion of crater ejecta deposits on Mars, *Icarus*, *27*, 503–516, 1976.

Baker, V. R., Water and the Martian landscape, *Nature*, *412*, 228–236, 2001.

Baker, V. R., and D. J. Milton, Erosion by catastrophic floods on Mars and Earth, *Icarus*, *23*, 27–41, 1974.

Baratoux, D., C. Delacourt, and P. Allemand, An instability mechanism in the formation of the Martian lobate craters and the implications for the rheology of ejecta, *Geophys. Res. Lett.*, *29*(8), 1210, doi:10.1029/2001GL013779, 2002.

Barlow, N. G., A new view of Martian impact craters, in *Large Meteorite Impact*, *Lunar and Planetary Institute Meetings*, Lunar Planet. Inst., Houston, Tex., abstract 4018, 2003.

Barlow, N. G., and T. L. Bradley, Martian impact craters: Correlations of ejecta and interior morphologies with diameter, latitude, and terrain, *Icarus*, *87*, 156–179, 1990.

Barlow, N. G., and A. Pollak, Comparisons of ejecta mobility ratios in the northern and southern hemispheres of Mars, *Lunar Planet. Sci.* [CD-ROM], *XXXIII*, abstract 1322, 2002.

Barlow, N. G., J. M. Boyce, F. M. Costard, R. A. Craddock, J. B. Garvin, S. E. H. Sakimoto, R. O. Kuzmin, D. J. Roddy, and L. A. Soderblom, Standardizing the nomenclature of Martian impact crater ejecta morphologies, *J. Geophys. Res.*, *105*, 26,733–26,738, 2000.

Bell, J. F., III, et al., Mineralogic and compositional properties of Martian soil and dust: Results from Mars Pathfinder, *J. Geophys. Res.*, *105*, 1721–1755, 2000.

Bennett, M., and N. Glasser, *Glacial Geology: Ice Sheets and Landforms*, John Wiley, Hoboken, N. J., 1996.

Böhlke, J. K., G. E. Ericksen, and K. Revesz, Stable isotope evidence for an atmospheric origin desert nitrate deposits in northern Chile and southern California, U.S.A., *Chem. Geol.*, *136*, 135–152, 1997.

Breed, C. S., J. F. McCauley, M. I. Whitney, V. P. Tchakarian, and J. E. Laity, Wind erosion in drylands, in *Arid Zone Geomorphology: Process, Form, and Change Drylands*, edited by D. S. G. Thomas, pp. 437–464, John Wiley, Hoboken, N. J., 1997.

Bulmer, M. H., L. Glaze, O. S. Barnouin-Jha, W. Murphy, and G. Neumann, Modelling mass movements for planetary studies, *Lunar Planet. Sci.*, *XXXIII*, abstract 1533, 2002.

Cabrol, N. A., and E. A. Grin, A morphological view on potential niches for exobiology on Mars, *Planet. Space Sci.*, *43*, 179–188, 1995.

Cabrol, N. A., E. A. Grin, and G. Dawidowicz, Ma'adim Vallis revisited through new topographic data: Evidence for an ancient intervalley lake, *Icarus*, *123*, 269–283, 1996.

Cabrol, N. A., E. A. Grin, and R. Landheim, Ma'adim Vallis evolution: Geometry and models of discharge rate, *Icarus*, *132*, 362–377, 1998a.

Cabrol, N. A., E. A. Grin, and R. Landheim, Ma'adim Vallis evolution: Geometry and models of discharge rate, *Icarus*, *132*, 362–377, 1998b.

Carr, M. H., The Martian drainage system and the origin of valley networks and fretted channels, *J. Geophys. Res.*, *100*, 7479–7507, 1995.

Carr, M. H., *Water on Mars*, Oxford Univ. Press, New York, 1996.

Carr, M. H., Elevations of water-worn features on Mars: Implications for circulation of groundwater, *J. Geophys. Res.*, *107*(E12), 5131, doi:10.1029/2002JE001845, 2002.

Carr, M. H., and G. D. Clow, Martian channels and valleys: Their characteristics, distribution and age, *Icarus*, *48*, 91–117, 1981.

Carr, M. H., and M. C. Malin, Meter-scale characteristics of Martian channels and valleys, *Icarus*, *146*, 366–386, 2000.

Cas, R. A. F., and J. V. Wright, *Volcanic Successions, Modern and Ancient: A Geological Approach to Processes, Products, and Successions*, Allen and Unwin, Concord, Mass., 1987.

Catling, D. C., A chemical model for evaporites on early Mars: Possible sedimentary tracers of the early climate and implications for exploration, *J. Geophys. Res.*, *104*, 16,453–16,470, 1999.

Christensen, P. R., Formation of recent Martian gullies through melting of extensive water-rich snow deposits, *Nature*, *422*, 45–48, 2003.

Christensen, P. R., et al., Miniature Thermal Emission Spectrometer for the Mars Exploration Rovers, *J. Geophys. Res.*, *108*(E12), 8064, doi:10.1029/2003JE002117, in press, 2003.

Clark, B. C., A. K. Baird, R. J. Weldon, D. M. Tsusaki, L. Schnabel, and M. P. Candelaria, Chemical composition of Martian fines, *J. Geophys. Res.*, *87*, 10,059–10,067, 1982.

Clifford, S. M., Polar basal melting on Mars, *J. Geophys. Res.*, *92*, 9135–9152, 1987.

Clifford, S. M., A model for the hydrologic and climatic behavior of water on Mars, *J. Geophys. Res.*, *98*, 10,973–11,016, 1993.

Clifford, S. M., and T. J. Parker, The evolution of the Martian hydrosphere: Implications for the fate of a primordial ocean and the current state of the northern plains, *Icarus*, *154*, 40–79, 2001.

Collinson, J. D., Alluvial sediments, in *Sedimentary Environments: Processes, Facies and Stratigraphy*, edited by H. G. Reading, pp. 37–82, Blackwell Sci., Malden, Mass., 1996.

Costard, F. M., The spatial distribution of volatiles in the Martian hydrolithosphere, *Earth Moon Planets*, *45*, 265–290, 1989.

DeHon, R. A., Martian sedimentary provinces, *Lunar Planet. Sci.*, *XXXII*, abstract 1361, 2001.

Dunkerley, D. L., and K. J. Brown, Desert soils, in *Arid Zone Geomorphology: Process, Form, and Change Drylands*, edited by D. S. G. Thomas, pp. 55–68, John Wiley, Hoboken, N. J., 1997.

Eriksen, G. E., Geology and origin of the Chilean nitrate deposits, *U.S. Geol. Surv. Prof. Pap.*, *1188*, 11 pp, 1981.

Eugster, H. P., and K. Kelts, Lacustrine chemical sediments, in *Chemical Sediments and Geomorphology*, edited by J. J. Gouldie and K. Pye, pp. 321–368, Academic, San Diego, Calif., 1983.

Farmer, J. D., Site selection, in *An Exobiological Strategy for Mars Exploration*, *Rep. SP 530,* pp. 42–50, NASA, U.S. Govt. Print Off., Washington, D. C., 1995.

Farmer, J. D., Hydrothermal processes on Mars: An assessment of present evidence, in *Evolution of Hydrothermal Ecosystems on Earth (and Mars?)*, edited by G. Bock and J. Goode, pp. 273–299, John Wiley, Hoboken, N. J., 1996.

Farmer, J. D., Taphonomic modes in microbial fossilization, in *Proceedings of the Workshop on Size Limits of Very Small Microorganisms*, *Space Studies Board*, *National Research Council*, pp. 94–102, Natl. Academy Press, Washington, D. C., 1999.

Farmer, J. D., Hydrothermal systems: Doorways to early biosphere evolution, *GSA Today*, *10*, 1–9, 2000a.

Farmer, J. D., Exploring for a fossil record of extraterrestrial life, in *Palaeobiology II*, edited by D. Briggs and P. Crowther, pp. 10–15, Blackwell Sci., Malden, Mass., 2000b.

Farmer, J. D., and D. J. Des Marais, Exploring for a record of ancient Martian life, *J. Geophys. Res.*, *104*, 26,977–26,995, 1999.

Fischer, R. V., and H. U. Schmincke, *Pyroclastic Rocks*, Springer-Verlag, New York, 1984.

Fournier, R. O., Geochemistry and dynamics of the Yellowstone National Park hydrothermal system, *Ann. Rev. Earth Planet. Sci.*, *17*, 13–53, 1989.

Frey, H., and R. A. Schultz, Large impact basins and the mega-impact origin for the crustal dichotomy on Mars, *Geophys. Res. Lett.*, *15*, 229–232, 1988.

Frey, H. V., J. H. Roark, K. M. Shockey, E. L. Frey, and S. E. H. Sakimoto, Ancient lowlands on Mars, *Geophys. Res. Lett.*, *29*(10), 1384, doi:10.1029/2001GL013832, 2002.

Fryberger, S. G., T. S. Ahlbrandt, and S. Andrews, Origin, sedimentary features, and significance of low-angle aeolian sand sheet deposits, Great Sand Dunes National Monument and vicinity, Colorado, *J. Sediment. Petrol.*, *49*, 733–746, 1979.

Garvin, J. B., and J. J. Frawley, Geometric properties of Martian impact craters: Preliminary results from the Mars Orbital Laser Altimeter, *Geophys. Res. Lett.*, *25*, 4405–4408, 1998.

Garvin, J. B., S. E. H. Sakimoto, J. J. Frawley, and C. Schnetzler, North polar region craterforms on Mars: Geometric characteristics from the Mars Orbiter Laser Altimeter, *Icarus*, *144*, 329–352, 2000.

Golombek, M., et al., Preliminary engineering constraints on potential landing sites for the Mars Exploration Rovers, *Proc. Lunar Planet. Sci. Conf., 32nd*, abstract 1234, 2001.

Greeley, R., and J. E. Guest, Geologic map of the eastern equatorial region of Mars, *U.S. Geol. Surv. Misc. Geol. Invest. Map, I-1802-B*, 1987.

Greeley, R., N. Lancaster, S. Lee, and P. Thomas, Martian aeolian processes, sediments, and features, in *Mars*, edited by H. H. Kiefer et al., pp. 730–766, Univ. Arizona Press, Tucson, 1992.

Greeley, R., R. O. Kuzmin, S. C. R. Rafkin, T. I. Michaels, and R. Haberle, Wind-related features in Gusev crater, Mars, *J. Geophys. Res.*, *108*(E12), 8087, doi:10.1029/2002JE002006, in press, 2003.

Grin, E. A., and N. A. Cabrol, Limnologic analysis of Gusev Crater paleolake, Mars, *Icarus*, *130*, 461–474, 1997.

Gulick, V. C., Magmatic intrusions and a hydrothermal origin for fluvial valleys on Mars, *J. Geophys. Res.*, *103*, 19,365–19,388, 1998.

Gunnlaugsson, H. P., G. Weyer, and Ö. Helgason, Titanomaghemite in Icelandic basalt: Possible clues for the strongly magnetic phases in Martian soil and dust, *Planet. Space Sci.*, *50*, 157–161, 2002.

Gutmann, J. T., Strombolian and effusive activity as precursors to phreatomagmatism: Eruptive sequences at maars of Pinacate volcanic field, Sonora, Mexico, *J. Volcanol. Geotherm. Res.*, *113*, 345–356, 2002.

Hagerty, J. J., and H. E. Newsom, New evidence for impact-induced hydrothermal alteration at the Lonar crater, India: Implications for the effect of small craters on the mineralogical and chemical composition of the Martian regolith, *Lunar Planet. Sci.*, *XXXII*, abstract 1131, 2001.

Hartmann, W. K., and G. Neukum, Cratering chronology and the evolution of Mars, *Space Sci. Rev.*, *96*, 165–194, 2001.

Hartmann, W. K., J. Anguita, M. A. de la Casa, D. C. Berman, and E. V. Ryan, Martian cratering 7: The role of impact gardening, *Icarus*, *149*, 37–53, 2001.

Hartmann, W. K., T. Thorsteinsson, and F. Sigurdsson, Comparison of Icelandic and Martian hillside, *Lunar Planet. Sci.*, *XXXIII*, abstract 1004, 2002.

Hoffman, N., White Mars: A new model for Mars' surface and atmosphere based on CO_2, *Icarus*, *146*, 326–343, 2000.

Hofmann, B. A., and J. D. Farmer, Filamentous fabrics in low-temperature mineral assemblages: Are they fossil biomarkers? Implications for the search for a subsurface fossil record on the early Earth and Mars, *Planet. Space Sci.*, *48*, 1077–1086, 2000.

Irwin, P. I., T. A. Maxwell, A. D. Howard, R. A. Craddock, and D. W. Leverington, A large paleolake basin at the head of Ma'adim Vallis, Mars, *Science*, *296*, 2209–2212, 2002.

Jakosky, B. M., and M. H. Carr, Possible precipitation of ice at low latitudes of Mars during periods of high-obliquity, *Nature*, *315*, 559–561, 1985.

Klein, C., and C. S. Hurlbut Jr., *Manuel of Mineralogy*, John Wiley, Hoboken, N. J., 1993.

Kuzmin, R. O., N. N. Bobina, E. V. Zabalueva, and V. P. Shashkina, Structural inhomogeneities of the Martian cryosphere, *Sol. Syst. Res.*, *22*, 121–133, 1988.

Kuzmin, R. O., R. Greely, R. Landheim, N. A. Cabrol, and J. D. Farmer, Geologic map of the MTM-15,182 and MTM-15,187 quadrangles, Gusev Crater-Ma'adim Vallis region, Mars, U.S, *Geol. Surv. Misc. Geol. Invest. Map*, *I-2666*, 2000.

Lee, P., C. McKay, and J. Matthews, Gullies on Mars: Clues to their formation timescale from possible analogs from Devon Island, Nunavut, arctic Canada, *Lunar Planet. Sci.*, *XXXIII*, abstract 2050, 2002.

Li, J., T. K. Lowenstein, C. B. Brown, T. Ku, and S. Luo, A 100 Ka record of water tables and paleoclimates from salt cores, Death Valley, California, *Palaeogeogr. Palaeoclimatol. Palaeoecol.*, *123*, 179–203, 1996.

Malin, M. C., and K. S. Edgett, Evidence for recent groundwater seepage and surface runoff on Mars, *Science*, *288*, 2330–2335, 2000a.

Malin, M. C., and K. S. Edgett, Sedimentary rocks of early Mars, *Science*, *290*, 1927–1937, 2000b.

Mangold, N., F. Costard, F. Forget, and J. P. Peulvast, Narrow gullies over high sand dunes on Mars: Evidence for flows triggered by liquid water near surface, *Lunar Planet. Sci.*, *XXXIII*, abstract 1215, 2002.

Masursky, H., An overview of geological results from Mariner 9, *J. Geophys. Res.*, *78*, 4009–4030, 1973.

McCarville, P. J., and L. J. Crossey, Post-impact hydrothermal alteration of the Manson impact structure, Manson, Iowa, in *The Manson Impact Structure*, *Spec. Pap. Geol. Soc. Am.*, *302*, 347–369, 1996.

McCauley, J. F., Mariner 9 evidence for wind erosion in the equatorial and mid-latitude regions of Mars, *J. Geophys. Res.*, *78*, 4123–4138, 1973.

McEwen, A. S., M. C. Malin, M. H. Carr, and W. K. Hartmann, Voluminous volcanism on early Mars revealed in Valles Marineris, *Nature*, *397*, 584–586, 1999.

McKay, C. P., G. D. Clow, R. A. Wharton, and S. S. Squyres, Thickness of ice on perennially frozen lakes, *Nature*, *313*, 561–562, 1985.

Melosh, H. J., *Impact Cratering: A Geologic Process*, 245 pp., Oxford Univ. Press, New York, 1989.

Milam, K. A., K. R. Stockstill, J. E. Moersch, H. Y. McSween Jr., L. L. Tornabene, A. Ghosh, M. B. Wyatt, and P. R. Christensen, THEMIS characterization of the MER Gusev crater landing site, *J. Geophys. Res.*, *108*(E12), 8078, doi:10.1029/2002JE002023, in press, 2003.

Mouginis-Mark, P., Martian fluidized crater morphology: Variations with crater size, latitude, altitude, and target material, *J. Geophys. Res.*, *84*, 8011–8022, 1979.

Mouginis-Mark, P., Ejecta emplacement and modes of formation of Martian fluidized ejecta craters, *Icarus*, *45*, 60–76, 1981.

Musselwhite, D. S., T. D. Swindle, and J. I. Lunine, Liquid CO_2 breakout and the formation of recent small gullies on Mars, *Geophys. Res. Lett.*, *28*, 1283–1285, 2001.

Newsom, H. E., Hydrothermal alteration of impact melt sheets with implications for Mars, *Icarus*, *44*, 207–216, 1980.

Newsom, H. E., J. J. Hagerty, and I. E. Thorsos, Location and sampling of aqueous and hydrothermal deposits in Martian impact craters, *Astrobiology*, *1*, 71–88, 2001.

Orton, G. J., Volcanic environments, in *Sedimentary Environments: Processes, Facies and Stratigraphy*, edited by H. G. Reading, pp. 485–567, Blackwell Sci., Malden, Mass., 1996.

Pye, K., *Aeolian Dust and Dust Deposits*, Academic, San Diego, Calif., 1987.

Ramstad, J. D., Quantitative comparison of pedestal and layered ejecta impact craters on Mars, M.S. thesis, Northern Arizona Univ., Flagstaff., 2001.

Rathbun, J. A., and S. W. Squyres, Hydrothermal systems associated with Martian impact craters, *Icarus*, *157*, 362–372, 2002.

Rieder, R., T. Economou, H. Wänke, A. Turkevich, J. Crisp, J. Brückner, G. Dreibus, and H. Y. McSween, The chemical composition of Martian soil and rocks returned by the mobile alpha proton X-ray spectrometer: Preliminary results from the X-ray mode, *Science*, *278*, 1771–1774, 1997.

Robinson, M. S., P. J. Mouginis-Mark, J. R. Zimbleman, S. S. C. Wu, K. K. Ablin, and A. E. Howington-Kraus, Chronology, eruption duration, and atmospheric contribution of the Martian volcano Apollinaris Patera, *Icarus*, *104*, 301–323, 1993.

Scott, D. H., and K. L. Tanaka, Geologic map of the western equatorial region of Mars, scale 1:15,000,000, *U.S. Geol. Surv. Misc. Geol. Invest. Map*, *I-1802-A*, 1986.

Sharp, R. P., and M. C. Malin, Channels on Mars, *Geol. Soc. Am. Bull.*, *86*, 593–609, 1975.

Shaw, P. A., and D. S. G. Thomas, Pans, playas, and salt lakes, in *Arid Zone Geomorphology*, edited by D. S. G. Thomas, pp. 293–317, John Wiley, Hoboken, N. J., 1997.

Squyres, S. W., et al., Athena Mars Rover science investigation, *J. Geophys. Res.*, *108*(E12), 8062, doi:10.1029/2003JE002121, in press, 2003.

Stewart, S. T., and F. Nimmo, Surface runoff features on Mars: Testing the carbon dioxide formation hypothesis, *Proc. Lunar Planet. Sci. Conf., 32nd*, abstract 1780, 2001.

Tanaka, K. L., The stratigraphy of Mars, Proc. Lunar Planet. Sci. Conf., 17th, Part 1, *J. Geophys. Res.*, *91*, suppl., E139–E158, 1986.

Tanaka, K. L., Dust and ice deposition in the Martian geologic record, *Icarus*, *144*, 254–266, 2000.

Tanaka, K. L., N. E. Isbell, D. H. Scott, R. Greeley, and J. E. Guest, The resurfacing history of Mars: A synthesis of digitized, Viking-based geology, *Proc. Lunar Planet. Sci. Conf.*, *18th*, 665–678, 1988.

Thorsos, I. E., H. E. Newsom, and A. D. Davies, Availability of heat to drive hydrothermal systems in large Martian impact craters, *Lunar Planet. Sci.*, *XXXII*, abstract 2011, 2001.

Witbeck, N. E., K. L. Tanaka, and D. H. Scott, Geologic map of the Valles Marineris region, Mars, *U.S. Geol. Surv. Misc. Geol. Invest. Map*, *I-2010*, 1991.

C. Barber, H. Newsom, and I. Thorsos, Institute of Meteoritics, Room 306D, Northrop Hall, University of New Mexico, Albuquerque, NM 87131, USA. (newsom@unm.edu; ivan.e.thorsos@jpl.nasa.gov)

N. G. Barlow, U.S. Geological Survey, 2255 North Gemini Drive, Flagstaff, AZ 86002, USA. (nadine.barlow@nau.edu)

N. A. Cabrol, E. A. Grin, J. M. Moore, and B. Sutter, NASA Ames Research Center, MS 245-3, Moffett Field, CA 94035-1000, USA. (ncabrol@mail.arc.nasa.gov; egrin@mail.arc.nasa.gov; jmoore@mail.arc.nasa.gov; bsutter@mail.arc.nasa.gov)

M. H. Carr, U.S. Geological Survey, Mail Stop 975, 345 Middlefield Road, Menlo Park, CA 94025-3591, USA. (carr@usgs.gov)

O. de Goursac, Mars Society en France, 10/16 Rue du Mont Valérien, F-92150 Suresnes, France. (goursac@club-internet.fr)

D. J. Des Marais, NASA Ames Research Center, MS 239-4, Moffett Field, CA 94035-1000, USA. (david_desmarais@qmgate.arc.nas)

J. D. Farmer, F. D. Grant, and R. Greeley, Department of Geological Sciences, Arizona State University, Box 871404, Tempe, AZ 85287-1404, USA. (jfarmer@asu.edu; greeley@asu.edu)

D. A. Fike, Department of Earth, Atmospheric, and Planetary Sciences, Massachussetts Institute of Technology, 77 Massachusetts Avenue, 54-812, Cambridge, MA 02139, USA. (ngb@physics.ucf.edu)

B. Grigsby, Schreder Planetarium, 1644 Magnolia Avenue, Redding, CA 96001, USA. (brian@projectarise.org)

M. G. Kramer, NASA Ames Research Center, MS 242-4, Moffett Field, CA 94035-1000, USA. (kramerm@fsl.orst.edu)

R. O. Kuzmin, Vernadsky Institute, Russian Academy of Sciences, Kosygin Street 19, Moscow 117975 GSP-1, Russia. (rok@geokhi.ru)

K. L. Tanaka, Department of Physics and Astronomy, Northern Arizona University, NAU Box 6010, Flagstaff, AZ 86011-6010, USA. (ktanaka@usgs.gov)

M. L. Urquhart, Department of Science and Mathematics Education, University of Texas at Dallas, FN 32, P.O. Box 830688, Richardson, TX 75083-0688, USA. (urquhart@utdallas.edu)